

Analysis of WAsP (Wind Atlas Analysis and Application Program) in complex topographical conditions using measured production from a large scale wind farm.

Stefan Sveinbjornsson

A thesis

submitted in partial fulfillment of the
requirements for the degree of
Master of Science in Civil Engineering

University of Washington

2013

Committee:

Timothy Larson

Joe Mahoney

Program Authorized to Offer Degree:

Department of Civil and Environmental Engineering

Contents

Table of Figures	3
Abstract	10
1. Introduction	11
2. Methods	14
2.1. Measured data from wind farm	14
2.2. Vestas V80 1.8 MW Turbines.....	15
2.3. Wind Atlas Analysis and Application Program (WAsP).....	16
2.3.1. Wind data analysis and projection	16
2.3.2. Topographical data.....	19
2.3.3. Power Production.....	21
2.3.4. Wake Effect modeling	21
2.3.5. Limitations of WAsP	24
3. Results	29
3.1. Topographical data input.....	29
3.2. Meteorological data.....	30
3.3. Net Annual Power production.....	31
3.3.1. WAsP AEP Predictions.....	31
3.3.2. Pre-Expansion AEP and Wake Losses	33
3.3.3. Empirical User Corrections.....	34
3.4. Wind Resource Grid.....	39
3.5. Measured Production vs. Predicted Production	41
3.5.1. Filtering the Measured Production.....	41
3.5.2. WAsP Predictions	42
3.5.3. Visual Comparison of Ruggedness Index.....	49
4. Discussion.....	53
4.1. Topographical Data Input.....	53
4.2. Meteorological Data.....	54
4.3. Net Annual Power Production.....	55

- 4.3.1. WAsP AEP Predictions..... 55
- 4.3.2. Empirical User Corrections..... 55
- 4.3.3. Pre-Expansion AEP and Wake Losses 56
- 4.4. Measured Production vs. Measured Production..... 57
 - 4.4.1. WAsP Predictions 57
 - 4.4.2. Empirical User Corrections..... 58
 - 4.4.3. Visual Comparison..... 60
- 4.5. Final Analysis..... 61
- 5. Conclusions 63
- Bibliography 65
- Appendix A - Predicted Production..... 68
 - WAsP Predictions 68
 - Overestimation of Wind Speeds due to roughness of terrain..... 71
 - Underestimation of Wind Speeds due to roughness of terrain..... 74
- Appendix B – Measured vs. Predicted Production 77
 - WAsP Predictions 77
 - Overestimation of Wind Speeds due to roughness of terrain..... 80
 - Underestimation of Wind Speeds due to roughness of terrain..... 83

Table of Figures

Figure 1- Estimated power production curve (blue) for a Vestas V 80 (1.8MW) wind turbine at a height of 67 meters and with air density of 1.225 kg/m³ at different wind speeds. Figure represents values used by WAsP to estimate power production. (WAsP, WAsP 10.2, 2012). 16

Figure 2 - Example of the output of an analyzed MET data of wind data in WAsP (WAsP, WAsP, 2012)..... 19

Figure 3- The projected turbine as seen in Google earth. The 3 dimensional projection is implemented by WAsP but the satellite imagery also shows the turbine. 21

Figure 4 - Example of how WAsP calculates wind turbine output at turbine downwind (WAsP, WAsP, 2012)..... 24

Figure 5 - The terrain surrounding a met. station site as seen in the WAsP Map Editor. Terrain steeper than a certain critical angle, is indicated by the thick red (radial) lines. The overall RIX value is simply the mean of the sector-wise RIX values (Mortensen, Bowen, & Antoniou, 2006). 26

Figure 6 - The topographical data map imported into WAsP. The red lines represent the elevation contour with 3m intervals and the other colored polygons are different roughness length classes. 29

Figure 7 - Wind Rose for the annual data collected at the MET and wind speed distribution (Weibull) for all sectors (wind directions) from WAsP..... 30

Figure 8 – Predicted Net AEP (GWh) and Wake Losses (%) for all wind farm sites..... 32

Figure 9 - Difference in production and wake losses for all 1.8 MW turbines. Wake loss difference is found by subtracting results from Pre-expansion analysis from WAsP Predictions with no user corrections. 34

Figure 10 – Predicted Net AEP (GWh) and Wake Losses (%) for all sites in wind farm with empirical correction applied for overestimation. 35

Figure 11 - Predicted Net AEP (GWh) and Wake Losses (%) for all turbine sites, with empirical correction applied for underestimations..... 37

Figure 12 - Resource Grid Map in WAsP showing the potential annual AEP for a 2.0 MW Vestas V80 Turbine within the wind farm boundary. 39

Figure 13 - Predicted Net AEP (GWh) and Wake Losses (%) for all turbine sites. Conditions from case 4 are used and 6 turbines that are relocated are circled (black). 40

Figure 14 - Changes in wake losses and AEP for all turbines due to the relocation of 6 turbines (Circled in black).	40
Figure 15 - Fraction of time available and Measured Power Production (GWh) for each turbine site.	42
Figure 16 - Scaled Predicted Production (GWh) and Measured Production (GWh) for all 1.8 MW sites.	43
Figure 17 - Scaled Predicted- and Measured Production for all 1.8 MW turbine sites.	44
Figure 18 – Histogram of the Deviation (%) of Scaled Predicted Production and Measured Production for all 1.8 MW Turbine Sites.	44
Figure 19 - Scaled Projected Production (GWh) and Measured Production (GWh) for all 1.8 MW sites, for one month. With empirical correction applied for overestimations.	45
Figure 20 - Scaled Predicted- and Measured Production for all 1.8 MW turbine sites. With empirical correction applied for overestimations.	46
Figure 21 - Histogram of the Deviation (%) of Scaled Predicted Production and Measured Production for all 1.8 MW Turbine Sites. With empirical correction applied for underestimations.	46
Figure 22- Scaled Predicted Production (GWh) and Measured Production (GWh) for all 1.8 MW sites, for one month. With empirical correction applied for underestimations.	47
Figure 23 - Scaled Projected- and Measured Production for all 1.8 MW turbine sites. With empirical correction applied for underestimations.	48
Figure 24 – Histogram of the Deviation (%) of Scaled Projected Production and Measured Production for all 1.8 MW Turbine Sites. With empirical correction applied for underestimations.	48
Figure 25 - 2.0 MW Turbine sites mapped with RIX and surface roughness polygons. Figure shows grid map of prevailing wind direction.	49
Figure 26- Turbine sites where WAsP overestimates production by 10% and over, mapped with RIX grid and surface roughness polygons. Figure shows grid maps of prevailing wind direction (bottom) and wind directions for sections 30° to either side (Top).	50
Figure 27 - Turbine sites where WAsP underestimates production by 10% and over, mapped with RIX grid and surface roughness polygons. Figure shows maps of prevailing wind direction (bottom) and wind directions for section 30° to either side (Top).	51

Figure 28 - Turbine sites where WAsP under/over- estimates production by less than 10%, mapped with RIX grid and surface roughness polygons. Figure shows maps of prevailing wind direction (bottom) and wind directions for section 30° to either side (Top).	52
Figure 29 - Wind Rose plotted from the yearly MET Data.	54
Figure 30 - Wind Roses from WAsP and monthly data, for 2 different turbine sites, distributed in different locations around the wind farm layout.	59
Figure 31 - All Turbine sites mapped with RIX averaged over all directions and surface roughness polygons.	61
Figure 32 – Net AEP (GWh) with elevation above sea level (m). No user corrections.	68
Figure 33 – Wake losses (% of gross AEP) with elevation above sea level (m). No user corrections.	68
Figure 34 – Net AEP (GWh) with Δ RIX (%).No user corrections.	69
Figure 35 – Wake losses (% of gross AEP) with Δ RIX(%). No user corrections.	69
Figure 36 - Δ RIX(%) with elevation above sea level (m). No user corrections.	70
Figure 37 - Net AEP (GWh) with elevation above sea level (m). User correction for overestimations applied.	71
Figure 38 – Wake losses (% of gross AEP) with elevation above sea level (m). User correction for overestimations applied.	71
Figure 39 – Net AEP (GWh) with Δ RIX (%). User correction for overestimations applied.	72
Figure 40 – Wake losses (% of gross AEP) with Δ RIX(%).User correction for overestimations applied.	72
Figure 41 - Δ RIX(%) with elevation above sea level (m). User correction for overestimations applied.	73
Figure 42 - Net AEP (GWh) with elevation above sea level (m). User correction for underestimations applied.	74
Figure 43 – Wake losses (% of gross AEP) with elevation above sea level (m). User correction for underestimations applied.	74
Figure 44 – Net AEP (GWh) with Δ RIX (%). User correction for underestimations applied.	75
Figure 45 – Wake losses (% of gross AEP) with Δ RIX(%). User correction for underestimations applied.	75

Figure 46 - Δ RIX(%) with elevation above sea level (m). User correction for underestimations applied.....	76
Figure 47 – Elevation above sea level (m) and Measured Production (GWh) for all 1.8 MW sites. No user corrections.	77
Figure 48 – Ruggedness Index (% of terrain exceeding critical slope) and Measured Production (GWh) for all 1.8 MW sites. No user corrections.	77
Figure 49 – Deviation of predicted from measured production (%) and elevation (m). No user corrections.	78
Figure 50 - Deviation of predicted from measured production (%) and Ruggedness Index (%).No user corrections.	78
Figure 51 - Deviation of predicted from measured production (%) and Distance from MET station (%). No user corrections.....	79
Figure 52 - Elevation above sea level (m) and Measured Production (GWh) for all 1.8 MW sites. User correction for overestimations applied.	80
Figure 53 - Ruggedness Index (% of terrain exceeding critical slope) and Measured Production (GWh) for all 1.8 MW sites. User correction for overestimations applied.....	80
Figure 54 - Elevation above sea level (m) and Measured Production (GWh) for all 1.8 MW sites. User correction for overestimations applied.	81
Figure 55 - Deviation of predicted from measured production (%) and Ruggedness Index (%). User correction for overestimations applied.	81
Figure 56 - Deviation of predicted from measured production (%) and Distance from MET station (%). User correction for overestimations applied.	82
Figure 57 - Elevation above sea level (m) and Measured Production (GWh) for all 1.8 MW sites. User correction for underestimations applied.	83
Figure 58 - Ruggedness Index (% of terrain exceeding critical slope) and Measured Production (GWh) for all 1.8 MW sites. User correction for underestimations applied.....	83
Figure 59 - Elevation above sea level (m) and Measured Production (GWh) for all 1.8 MW sites. User correction for underestimations applied.	84
Figure 60 - Deviation of predicted from measured production (%) and Ruggedness Index (%).User correction for underestimations applied.	84

Figure 61 - Deviation of predicted from measured production (%) and Distance from MET station (%). User correction for underestimations applied. 85

Table 1 - Results from the observed wind climate in WAsP. The emergent wind speeds are the weighted sums of the Weibull distributions in all directions..... 30

Table 2 - Annual Values for production, measured on-site..... 31

Table 3- Predictions from WAsP..... 32

Table 4 - Correlation between different factors in WAsP for all turbines..... 33

Table 5 - Correlation between different factors in WAsP for 1.8 MW turbines. 33

Table 6 - Correlation between different factors in WAsP for 2.0 MW turbines. 33

Table 7 - Predictions for Pre-expansion analysis in WAsP. 34

Table 8 - Predictions from WAsP with empirical correction applied for overestimation. 36

Table 9 - Correlation between different factors in WAsP for all turbines with empirical correction applied for overestimation. 36

Table 10- Correlation between different factors in WAsP for all 1.8 MW turbines with empirical correction applied for overestimation. 36

Table 11 - Correlation between different factors in WAsP for all 2.0 MW turbines, with empirical correction applied for overestimation. 36

Table 12 - Predictions from WAsP with empirical correction applied for underestimations..... 37

Table 13 - Correlation between different factors in WAsP for all turbines, with empirical correction applied for underestimations..... 38

Table 14- Correlation between different factors in WAsP for all 1.8 MW turbines, with empirical correction applied for underestimations..... 38

Table 15 - Correlation between different factors in WAsP for all 2.0 MW turbines, with empirical correction applied for underestimations. 38

Table 16 - Correlation Results for Measured Production. 43

Table 17 - Correlation of Deviation..... 43

Table 18 - Correlation Results for Measured Production. With empirical correction applied for overestimations. 45

Table 19 - Correlation Results for Measured Production. With empirical correction applied for underestimations. 47

Abstract

The wind energy industry is leading the charge for renewable energy in the United States. In 2012, 13,124 MW of wind power capacity was installed, almost double that of 2011. The micro-model analysis of wind farms in the pre-construction phase is vital to ensure the feasibility of every project. As wind farms take advantage of increased wind speeds due to complex topographical features, their modeling becomes more complicated and expensive. WAsP is a linear numerical model that has become an industry standard for wind farm siting in Europe. It uses topographical inputs along with on-site meteorology data, to project wind speed and direction, over a pre-defined grid. The accuracy of WAsP was examined for both un-edited and WAsP recommended user-defined alterations to the wind speed at hub height, at all sites. The unedited projections yielded the lowest deviations for the net annual production (-1.2%), whereas user corrections significantly over or underestimated power production. Some sites within the wind farm layout had over-estimations of wind speed, both due to ruggedness of the terrain and close proximity to forests. WAsP shows significant promise in projections across the grid layout. A combination of unedited and user corrections is recommended for future analysis for wind farm siting.

1. Introduction

The wind energy industry is leading the charge for renewable energy in the United States. In 2012, 13,124 MW of wind power capacity was installed, almost double that of 2011 (AWEA, 2013). Overall new wind energy capacity was just over 40% of all installed capacity in 2012, more than both coal and natural gas (FERC, Federal Energy Regulatory Commission, 2012). In January 2013, wind accounted for 77% of newly installed capacity, with solar contributing the other 23% (FERC, Federal Energy Regulation Commission, 2013). This increase can be attributed to improvements in technology, cost reduction and government strategies in relation to wind energy. Wind energy production is expected to increase as fuel costs continue to increase and environmental regulations call for reduction in greenhouse gas emissions (EIA, 2012).

In order to remain competitive, the cost of wind energy production must be reduced and kept at competitive prices.

There are numerous factors which can aid in reducing costs in wind farms, several of which must be performed before any hubs are constructed. The two most important factors are site selection and the site layout design (Walford, 2006). Although wind resource data provided by such institutions as the National Renewable Energy Laboratory (NREL), help to locate potentially feasible wind farm sites, the data available is interpolated between sites resulting in less than desired resolution. This hypothesis is supported in Hermann Hermannsson's thesis, where wind energy prediction software is compared against production data from a wind farm. The programs use data from NREL or stations located away from the wind farm. The extrapolation of wind data results in an underestimation of wind speed and therefore energy production at the site in question (Hermannsson, 2012). These results highlight the importance for micro scale numerical models to estimate wind speed and power production for a potential wind farm site.

When a desired site is analyzed, meteorological (MET) towers are installed at site to measure wind speed and wind direction over a time period of at least one year. When onsite measurements have been collected and adjusted, numerical models can analyze the results and predict the wind climate from the probability of the data. As with any data, longer records and records from several sites scattered around the potential wind farm can only increase the accuracy of the probabilities and therefore improve the estimations of the numerical models.

One of these models is called the Wind Atlas Analysis and Application Program or WAsP for short. This program was developed by the Technical University of Denmark (DTU) in 1987 and is constantly in development to improve the performance of the model, in particular when dealing with complex terrain and atmosphere (Mortensen, Heathfield, Myllerup, Landberg, & Rathmann, 2007). WAsP has become the industry standard for wind resource assessment and siting of wind turbines and wind farms (WAsP, WAsP, 2012). This linear numerical model can be used to assess crucial features of a wind farm. It can analyze wind data and project it over areas of similar climate to its reference site. The program accounts for obstacles, surface roughness and orography in its analyses (Bowen & Mortensen, 2004). WAsP can estimate the power production of single turbine site and for an entire wind farm. The model takes into account wake losses, layout and many other factors.

WAsP is an essential tool for use in pre-construction analyses of a wind farm and during its operational period. Using it correctly allows its user to identify a feasible location for new development or for expansion of current capacity.

In this thesis WAsP will be used to analyze the production of an operational wind farm of about 150 wind turbines. MET data collected over a one year period will be used to project wind speed and direction at each turbine site. Estimated production will be assessed by comparing it against

operational production data from the wind farm, for both individual turbines and total wind farm production. The main factors contributing to power loss will be analyzed and discussed. The overall accuracy of WAsP predictions will be discussed and whether it is a useful tool for a wind farm resource assessment for this particular wind farm.

2. Methods

As the number of wind energy projects increases, developers seek new locations for their projects or new sites for expansion of existing wind farms. These sites can be located in complex terrain or within an area that has not yet been investigated. In order to determine the feasibility of these sites, a pre-construction analysis must be performed and most likely a numerical computer model will be used. The complexities of these projects increase the risk of investment. In order to decide which projects to select and on what grounds, two factors have become very important; economy and wind farm capacity of power production. The numerical models are able to estimate the power production by considering several physical factors. The state of atmosphere can be described by the following seven variables: pressure, temperature, density, moisture, two horizontal velocity components; all function of time and position (Petersen, Mortensen, Landberg, Højstrup, & Frank, 1997). These seven variables can best be described by seven equations: the equation of state, the first law of thermodynamics, three components of Newton's second law, and the continuity equations for mass and substances. Mathematical models of the atmosphere can be obtained by integrating the relevant equations with special initial and boundary conditions. The models solve these equations by numerically forward marching in time, using the time rates of change of the variables, the derivative are replaced by ratio of finite differences and changes of the variables over a certain time interval are computed repeatedly as long as needed to acquire an estimate of acceptable accuracy. The atmosphere contains motions with scales varying from 1mm to thousands of kilometers. The optimal model should be constructed using the smallest spatial and temporal scale, however that requires significant computer power which can be both expensive and time consuming. As the computer power increases, these scales can become smaller and smaller, making the analyzes more accurate.

WAsP is a program which uses many of these mathematical models to analyze data and uses it to predict wind power production. WAsP is programmed for use with a standard PC and it's easily available. In this chapter the methods/models WAsP uses to convert MET data and topographical data into estimated power production will be discussed.

2.1.Measured data from wind farm

The wind farm has been operational since 2007 and has about 150 turbines. The turbines used are all from Vestas, a well-established manufacturer. The hub height of each turbine is 67 meters and their nominal output ranges from 1.8 to 2.0 MW. For these analyses only the data for sites with 1.8 MW turbines is available, there are currently over 100 turbines with available records. At each turbine site a sensor located at hub height records the vector average wind speed and direction every 10 minutes. For each turbine the power production over the 10 minute interval is recorded. The available data is will be used for analysis of accuracy of WAsP predicted results. There are two MET towers in operation within the boundaries of the wind farm. They record the 10 minute average wind speed and direction at a height of 67 meters. However, data is only available from one of these towers. The MET data will be used by WAsP for projection of wind speed and direction over the selected area. The wind speed and direction is then used by WAsP to estimate wind speed and direction over a user defined area, which is used at each turbine site within the wind farm. The data recorded at the MET tower has a range of one year.

2.2.Vestas V80 1.8 MW Turbines

The Vestas turbines have established themselves as a premier brand within the wind energy industry. The V80 turbines have a rotor diameter of 80 meters and have a hub height of 67 meters at this particular wind farm. It has a nominal output of 1.8 MW. It has cut in wind speed

of 4 m/s, a cut out wind speed of 25 m/s. At 15 m/s it reaches its maximum output (Vestas, 2005). The power curve used by WAsP for these turbines in its predictions can be seen in Figure 1. These numbers are provided by Vestas.

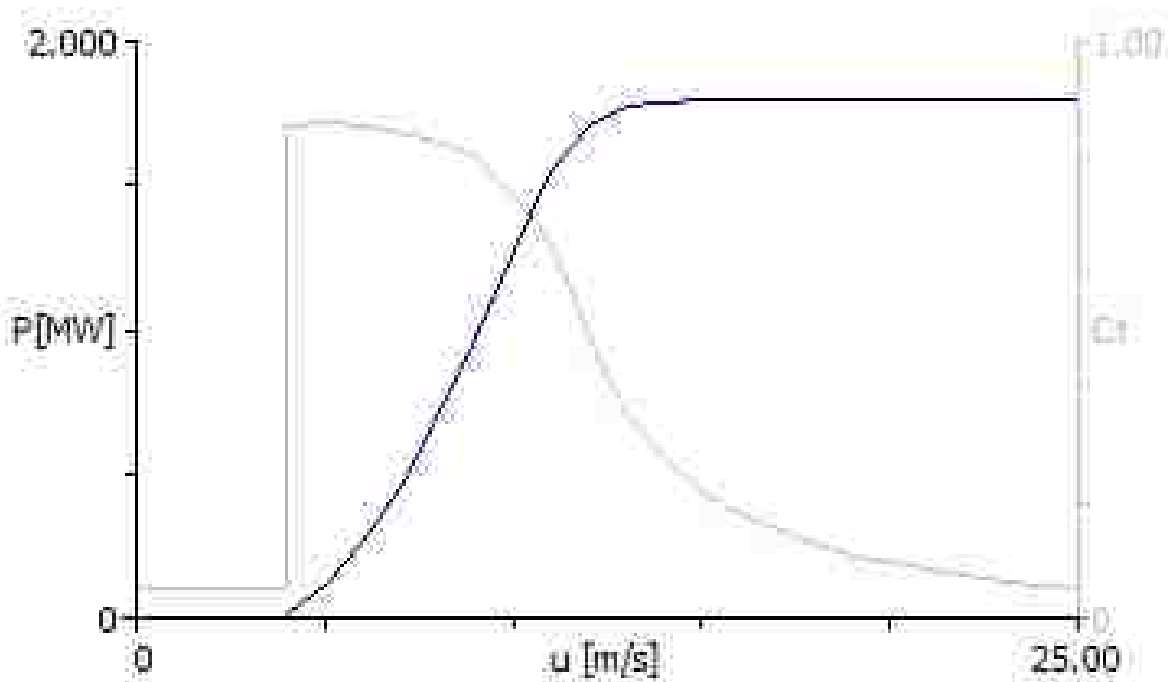


Figure 1- Estimated power production curve (blue) for a Vestas V 80 (1.8MW) wind turbine at a height of 67 meters and with air density of 1.225 kg/m^3 at different wind speeds. Figure represents values used by WAsP to estimate power production. (WAsP, WAsP 10.2, 2012).

2.3. Wind Atlas Analysis and Application Program (WAsP)

The numerical model was first developed in 1987 by the Department of Wind Energy at the Technical University of Denmark. It was developed for the analyses presented in the European Wind Atlas. The program employs a comprehensive list of models for projection of the horizontal and vertical extrapolation of wind climate statistics (Department of Wind Energy, 2012), the estimation of wind climate and wind resources (Frank, Rathmann, Mortensen, &

Landberg, 2001). The WAsP model is a linear numerical model which is based on the physical principles of flows in the atmospheric boundary layer. The model has been validated by a number of comparisons between measured and modeled wind statistics and wind farm production (Miljødata, 2002). The program is capable of describing wind flow over different terrains, close to sheltering obstacles and at specific points.

2.3.1. Wind data analysis and projection

Before the WAsP can project and estimate wind speeds, direction and power production at chosen locations, the provided wind data has to be analyzed. The 10 minute wind measurements described in chapter 2.1 is analyzed and a statistical summary of the observed, site specific wind climate is calculated. The output is a wind rose and the wind speed distributions in different sectors. A Weibull distribution function is then fitted to the measured histogram to provide scale and shape parameters A and k for each sector (see Figure 2). The Weibull distribution is well established for use with wind statistics as the natural distribution often fits the Weibull shape (Seguro & Lambert, Volume 85, Issue 1, March 2000).

The observed wind data is converted into a generalized wind climate or wind atlas data set shown in Figure 2. The wind observations have been cleaned with respect to site conditions such as: shelter (buildings etc.), surface roughness and orography. This information was acquired from different sources and was then converted into a map format which is readable by WAsP. The program used for conversion was Global Mapper™. When the data has been converted into standard conditions, e.g. transformed into Weibull A -and k - parameters for four standard roughnesses, five standard heights above ground and 12 azimuth sectors, it can then create a general wind atlas. (Frank, Rathmann, Mortensen, & Landberg, 2001). When the wind atlas data

has been generated, WAsP can estimate the wind climate at any particular point by performing the inverse calculation as is used to generate the wind atlas. The process can be simplified as:

discrete wind measurements → *wind statistics*

wind statistics + MET. Site description → *wind atlas data, generalized wind climate*

The WAsP wind flow model is based off the Jackson-Hunt theory (Troen, 1990). It solves the linearized Navier-Stokes equations by using several assumptions. The model assumes a steady state flow, linear advection and first order turbulence closure (Truepower, 2010).

WAsP uses the logarithmic wind profile to calculate the wind speed variance with height. It therefore considers three variables, the height above ground, the roughness length and friction velocity (Petersen, Mortensen, Landberg, Højstrup, & Frank, 1997). The roughness length parameterizes the roughness of the surface and the friction velocity parameterizes the frictional force between the moving air and ground. WAsP assumes that the atmosphere is stable and the balance between the flow is in equilibrium with the pressure force and the Coriolis force. (Petersen, Mortensen, Landberg, Højstrup, & Frank, 1997). WAsP uses the measured wind statistics and the surface roughness length around the MET station to calculate the geostrophic wind. This is modeled by calculating the friction velocity from the logarithmic wind profile and then applied in the geostrophic drag law to calculate the geostrophic wind.

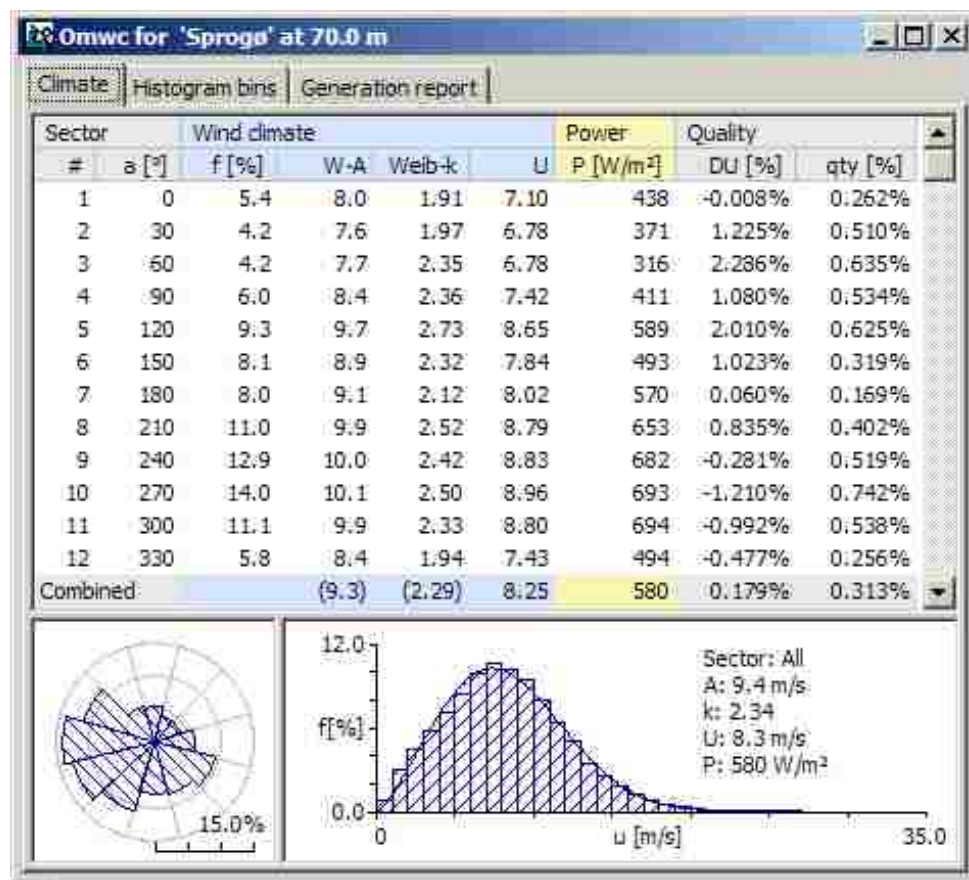


Figure 2 - Example of the output of an analyzed MET data of wind data in WAsP (WAsP, WAsP, 2012).

The double extrapolation method allows the model to use climate of the surface heat flux as a parameter for vertical extrapolation of wind. This allows the model to account for the deviations from the logarithmic profile which occurs often. These deviations are caused by the effect of buoyancy forces in the turbulence dynamics. This deviation is accounted for in simple model which uses the climatological average and root-mean-square of the surface heat flux. This helps account for the deviation by stability effects to the logarithmic wind profile when different conditions are calculated for heights and surfaces. The model includes a roughness change model which calculates the effect on the wind from topographical features, allowing it to calculate the

effect of changes between roughness lengths and height variations in the terrain (Petersen, Mortensen, Landberg, Højstrup, & Frank, 1997).

2.3.2. Topographical data

WAsP uses site specific topographical data to generalize the regional wind climatology and then uses the inverse calculation to acquire the projected wind climatology at a specific location. It is important that the topographical data is of sufficient accuracy to minimize uncertainty of wind speed projections.

The United States Geological Survey (USGS) has 10 meter spatial scale digital elevation models (DEM) of the wind farm area. This information was imported into a Geographical Information System (GIS) program which can export the information into a format readable by WAsP. WAsP requires this information to be exported as elevation contour lines. The contour lines had intervals of 3 meters which is recommended by WAsP (WAsP, WAsP 10.2, 2012).

The surface roughness lengths are determined by the land cover information. This data is available in a 30 meter resolution from the U.S. National Land Cover Database (NLCD) from 2006. Different surface lengths are given to different land covers. The same GIS program combines the DEM and Land Cover files in the same coordinate system. A readable WAsP spatial map file was then exported and used for analysis. The locations of turbines were determined by using Google Maps©. The accuracy of the projected turbine placements can be seen in Figure 3. WAsP has recently updated their program to project spatial maps into Google earth. When Figure 3 is analyzed, the wind turbine location is accurate and will not skew the results. The area of the map that was imported into WAsP and analyzed included the whole wind farm and roughly 5 kilometers from the edge of all turbines in all directions.



Figure 3- The projected turbine as seen in Google earth. The 3 dimensional projection is implemented by WAsP but the satellite imagery also shows the turbine.

2.3.3. Power Production

When WAsP has created a generalized wind climate for area, it uses the total energy content of the mean wind it has calculated from the MET data. With the provided Vestas turbine power curve it can estimate the annual energy production (AEP) at each of the turbines in the wind farm layout. The thrust coefficient curves of the turbine and the wind farm layout are then used to estimate the wake losses for each turbine. The net annual energy can then be estimated (WAsP, WAsP 10.2, 2012).

This can be express more simply as:

At each turbine site

generalized wind climate + site description → predicted wind climate

predicted wind climate + power curve → annual energy production (AEP) of wind turbine

For the entire wind farm:

predicted wind climates + wind turbine generator characteristics → gross annual energy production of wind farm

predicted wind climates + wind turbine generator characteristics + wind farm layout → wind farm wake losses

gross annual energy productions + wake losses → net annual energy production of wind farm

When these estimations have been calculated, they will be compared to the annual wind farm production. The predictions for original wind farm layout (with 1.8 MW turbines only) and expanded section (2.0 MW turbine sites) will also be compared to annual measurements. For each turbine the net annual energy production (AEP) will be used for comparisons with measured data.

Any significant discrepancies will be located and analyzed to determine the factors contributing to them.

The program is able to generate a wind resource grid displayed as a map over a selected area. These resource grid map allows the user to locate high yielding energy locations. If a turbine is producing significantly below average, with minute wake losses, than a more desirable site can be located and production for the modified wind farm can be estimated. The analysis in this thesis will focus on the initial predictions by WASP, with no user correction applied to the turbine sites. The effects of the complex terrain on the wind speed prediction will be investigated. It will be determined whether the terrain causes over or under-estimations of the AEP and if the empirical alterations can correct them.

2.3.4. Wake Effect modeling

WAsP models the estimated power loss in wind farms due to the wind speed reduction in wakes from up-wind turbines (Rathmann, Barthelmie, & Frandsen, 2006). This is a very important feature for wind farm analysis. A placement in a low wind speed location will produce very little power and placing a turbine within the proximity of another turbine can significantly lower the production at one of the sites due to wake effects.

WAsP implements the Park model to estimate wake effects and their effects on power production. The Park model is a computationally fast model which makes some simplifications in its estimations. The program assumes an initial loss in velocity behind the turbine rotor, calculated from the turbines thrust coefficient curve and an empirically determined wake-decay constant (Truepower, 2010). It simplifies the calculation by neglecting certain details in near-flow-field around a turbine rotor and by assuming the wakes to expand linearly with distance (WAsP, WAsP 10.2, 2012) (Rathmann, Barthelmie, & Frandsen, 2006). The Park model assumes the flow follows the terrain (Truepower, 2010). When there are multiple wakes it superimposes the wake cross sections of the upstream turbines. The projected wind speed at a downwind turbine is estimated as the free stream wind speed minus wake effects.

The wind speed deficit due to wake effects is then calculated downwind by using:

$$\delta V_{01} = U_0(1 - \sqrt{1 - C_t}) \left(\frac{D_0}{D_0 + 2kX_{01}} \right)^2 \frac{A_{overlap}}{A_1^{(R)}}$$

U_0 is the undisturbed wind speed at the up wind turbine (see Figure 4) with rotor diameter D_0 and k is the wake coefficient (Mortensen, Bowen, & Antoniou, 2006).

The wake loss in the prevailing wind direction will be used from WAsP for comparison where there is significant discrepancy between predicted and measured data.

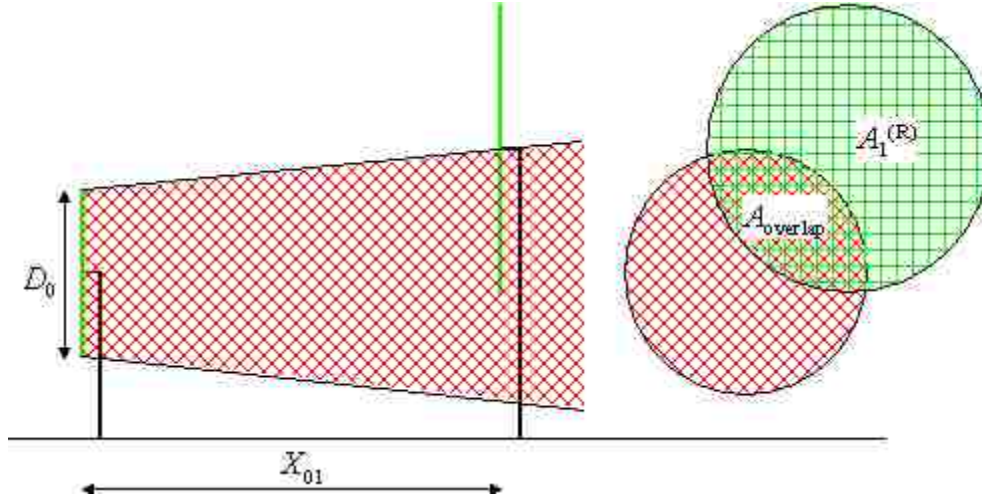


Figure 4 - Example of how WAsP calculates wind turbine output at turbine downwind (WAsP, WAsP, 2012).

2.3.5. Limitations of WAsP

Due to some of the simplifications made in the numerical models used within WAsP, the program can produce somewhat inaccurate results when used outside its recommended operational envelope (Bowen & Mortensen, 2004). When a site has complex, rugged terrain or very complex atmospheric conditions, the accuracy of WAsP can be unreliable (Mortensen, Bowen, & Antoniou, 2006). WAsP analyzes the orography and the site ruggedness index (RIX) of the entire grid layout. The associated performance indicator (ΔRIX) can identify problematic sites within a project. RIX is defined as the fractional extent of the surrounding terrain which is steeper than a critical slope, which is within the operational envelope of the WAsP flow model (Bowen & Mortensen, 2006). ΔRIX is defined as the difference in the (percentage) fractions between the predicted and reference sites (Bowen & Mortensen, 2004).

This problem can be solved by using several reference sites and cross-referencing sites where wind observations are available. There is also the option for some user corrections at problematic

sites which can significantly improve the accuracy of the model in complex terrain. (Mortensen, Bowen, & Antoniou, 2006). This method to uses ΔRIX to calculate a correction factor, which can then be inserted into WAsP to reduce/increase the wind speed at hub height at each turbine site.

The formula was derived from a study, using several sited to derive a relationship between ΔRIX and the estimation error of wind speeds. The formula derived is:

$$U_m = \frac{1}{\exp(\alpha \Delta RIX)} U_p$$

Where U_p is the projected wind speed at hub height and α is the number derived in Mortensen et al, 2006.

Where there is a significant difference in the measured and predicted AEP, the RIX and ΔRIX will be analyzed to evaluate its correlation with projection errors.

WAsP has also been known to have issues in projections near extensive forests, it tends to overestimate wind speed at these sites (Dellwik, Landberg, & Jensen, 2006).

More recently the wind energy industry has been trying to implement the use of Computational Fluid Dynamics (CFM) models for use in the wind energy industry. These models develop a steady-state, time-independent solution for the wind and turbulence field (Berge, Gravidahl, Schelling, Tallhaug, & Undheim, 2006). They solve the mass and momentum conservation of the Navier-Stokes equations (Beaucage, 2012). This is a physically more accurate modeling of the flow field when compared to WAsP.

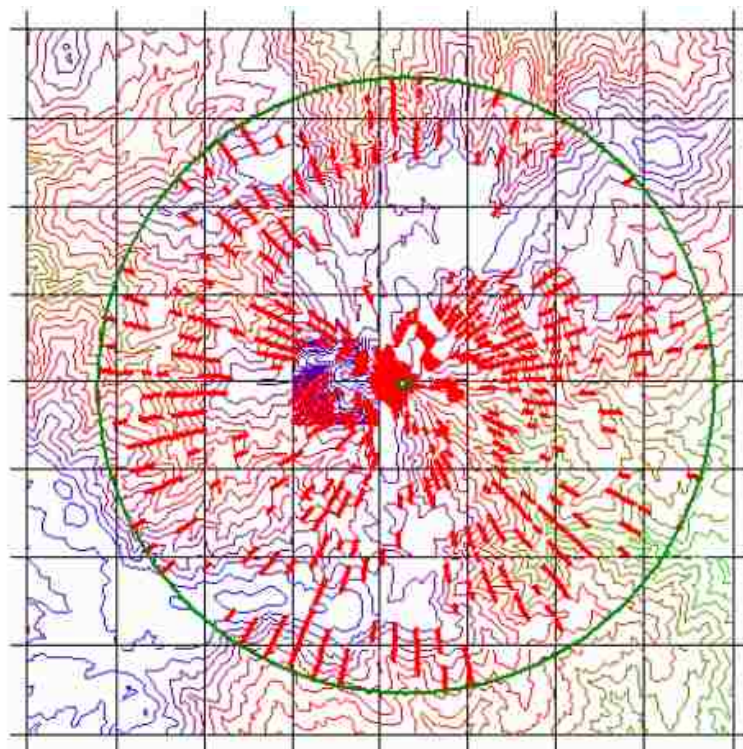


Figure 5 - The terrain surrounding a met. station site as seen in the WASP Map Editor. Terrain steeper than a certain critical angle, is indicated by the thick red (radial) lines. The overall RIX value is simply the mean of the sector-wise RIX values (Mortensen, Bowen, & Antoniou, 2006).

There have been several studies where WASP has been compared to CFD-models in complex terrains. These studies show that using CFD-models offers an improvement in some cases but not for all. (Berge, Gravdahl, Schelling, Tallhaug, & Undheim, 2006) (Periera & Guedes, 2006) (VanLuvanee, Rogers, Randall, Williamson, & Miller, 2009) (Sumner, Sibuet Watters, & Masson, 2010) (Beaucage, 2012). These CFD-models are very complicated and require significant computer power. It takes super computers several hours to complete the required calculations (Corbett, Ott, & Landberg, 2007).

Overall the WASP models perform adequately when operated within its envelope and even slightly outside it. CFD-models will inevitably be the industry standard but that seems to be decades away in the current computer power climate. WASP will continue to improve and adopt

new modeling techniques, helping it adapt for use in more complex terrain. As wind projects move to more complex terrain to take advantage of the high speed areas due to its terrain the importance for fast CFD-models will increase. For this project many factors projected by WAsP for this particular wind farm will be analyzed and compared to real 10 minute intervals of wind speed and power production. This will allow us to draw the conclusion of the accuracy for WAsP for the wind farm in question.

3. Results

3.1. Topographical data input

After importing topographical data map of the region into WAsP, the following map is produced. It has contour intervals of 3 meters and different surface roughness length polygons are assigned according to land use. This map seen in Figure 6 is used for all different cases using WAsP. The high density of red lines indicates a complex terrain with step elevation changes. This is confirmed by the high RIX values at several turbine sites.

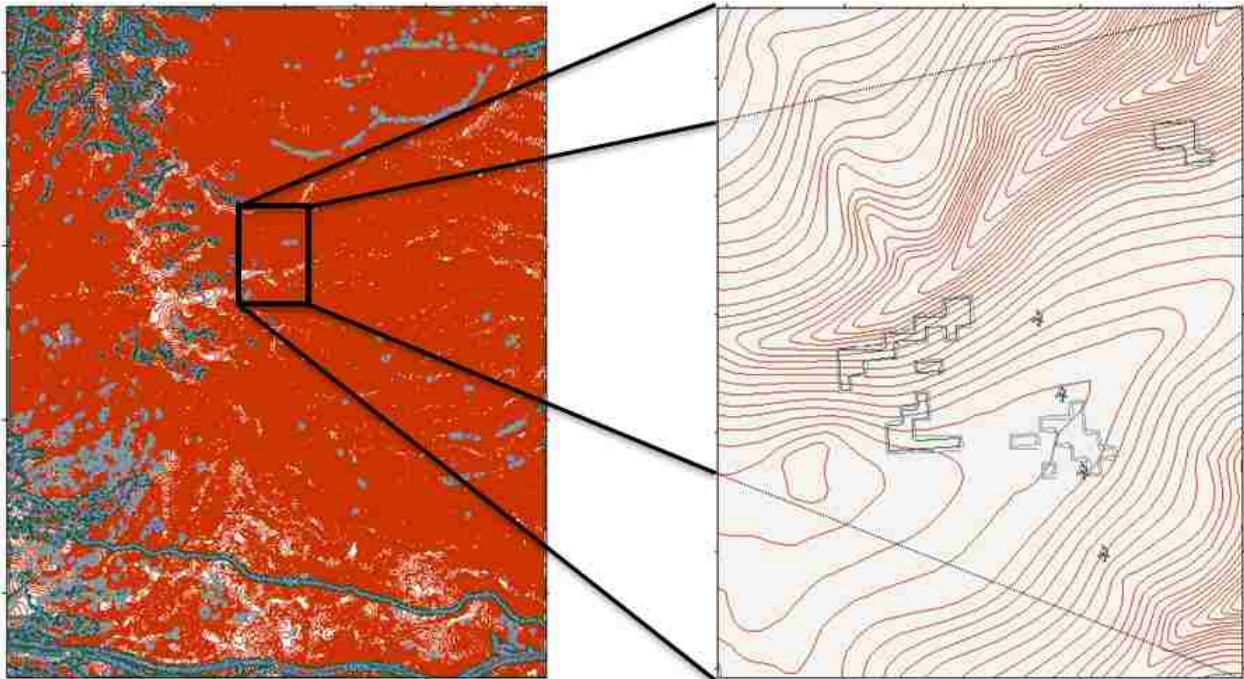


Figure 6 - The topographical data map imported into WAsP. The red lines represent the elevation contour with 3m intervals and the other colored polygons are different roughness length classes.

3.2.Meteorological data

After taking into account the topography factors, the following results are attained for the annual data, including wind speed and direction collected at the MET tower. The MET data included 10 minute average of wind speed and direction.

Table 1 - Results from the observed wind climate in WASP. The emergent wind speeds are the weighted sums of the Weibull distributions in all directions.

Parameter	Measured	Emergent	Discrepancy
Mean wind speed [m/s]	6.88	6.69	-2.6%
Mean power density [W/m ²]	492	493	0.2%

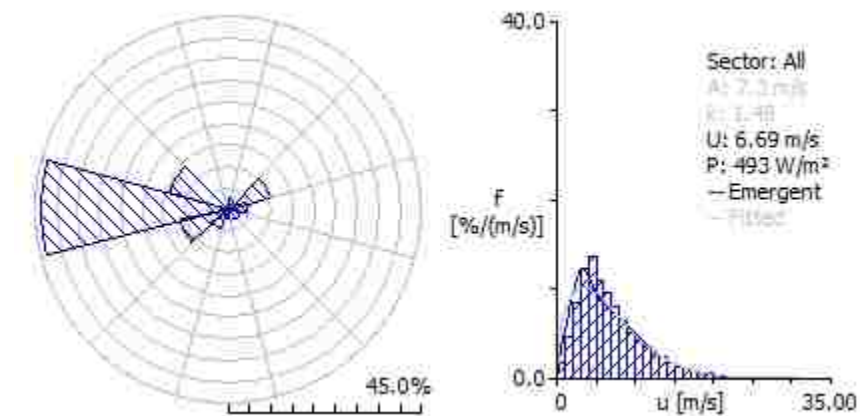


Figure 7 - Wind Rose for the annual data collected at the MET and wind speed distribution (Weibull) for all sectors (wind directions) from WASP.

These results are used for projection over the wind farm, using the topographical map and location and the selected wind turbine characteristics. The prevailing wind direction is definitively from east to west. All obstructions upwind in this direction will contribute significantly to wake losses at the wind farm.

3.3. Net Annual Power production

The wind speed is predicted at hub height for each turbine site and the power production can then be estimated. The predictions for all turbines will be presented and separate results for 1.8MW and 2.0MW turbine sites. The results shown are a summary for all wind directions.

The measured AEP from the wind farm is summarized in **Error! Not a valid bookmark self-reference.** It includes the availability of turbines and average AEP per turbine.

Table 2 - Annual Values for production, measured on-site.

	Measured AEP (GWh)	Average AEP per turbine (GWh)	Availability (%)
For 1.8 MW Turbines	635,575	5.005	97.60
For 2.0 MW Turbines	97,435	4.429	98.00
For All turbines	733,010	4.912	97.66

3.3.1. WAsP AEP Predictions

WAsP is used to predict the AEP without any user alterations. Figure 8 has the wake losses plotted against the net AEP, showing some correlation as is noted in Table 4.

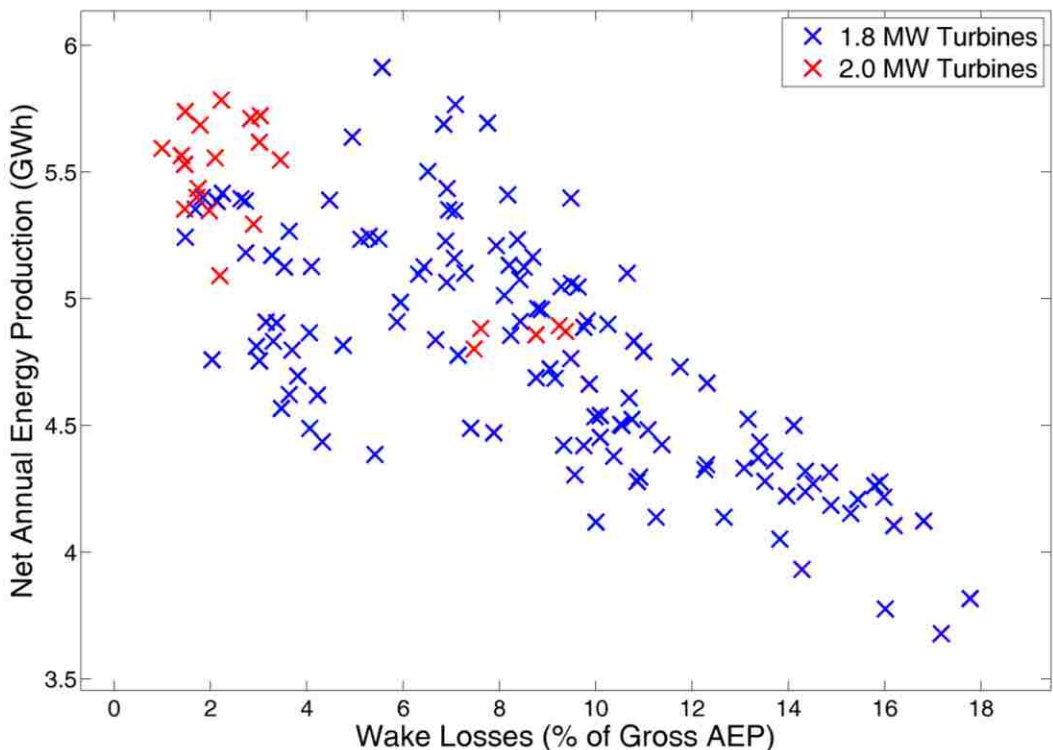


Figure 8 – Predicted Net AEP (GWh) and Wake Losses (%) for all wind farm sites.

The summarized result for the WASP predictions and the deviation from the measured AEP from The wind speed is predicted at hub height for each turbine site and the power production can then be estimated. The predictions for all turbines will be presented and separate results for 1.8MW and 2.0MW turbine sites. The results shown are a summary for all wind directions.

The measured AEP from the wind farm is summarized in **Error! Not a valid bookmark self-reference..** It includes the availability of turbines and average AEP per turbine.

Table 2 are located in Table 3.

Table 3- Predictions from WASP.

	Net AEP (GWh)	Average AEP per turbine (GWh)	Wake Loss (%)	Deviation from measured production (%)	Average ΔRIX (%)
For 1.8 MW	606.018	4.772	8.64	-4.65	4.06

Turbines					
For 2.0 MW Turbines	118.278	5.376	3.49	21.39	5.72
For All turbines	724.296	4.861	7.84	-1.19	4.31

In order to determine which factors within the model affect the predictions, the correlations between several factors are summarized in Table 4 to Table 6.

Table 4 - Correlation between different factors in WAsP for all turbines.

	Net AEP	Wake Losses	Elevation	ΔRIX
Net AEP	0.00	-0.77	0.25	-0.06
Wake Losses	-0.77	0.00	-0.25	0.36
Elevation	0.25	-0.25	0.00	-0.42
ΔRIX	-0.06	0.36	-0.42	0.00

Table 5 - Correlation between different factors in WAsP for 1.8 MW turbines.

	Net AEP	Wake Losses	Elevation	ΔRIX
Net AEP	0.00	-0.71	0.02	-0.15
Wake Losses	-0.71	0.00	-0.27	0.50
Elevation	0.02	-0.27	0.00	-0.60
ΔRIX	-0.15	0.50	-0.60	0.00

Table 6 - Correlation between different factors in WAsP for 2.0 MW turbines.

	Net AEP	Wake Losses	Elevation	ΔRIX
Net AEP	0.00	-0.83	0.97	-0.50
Wake Losses	-0.83	0.00	-0.40	0.68
Elevation	0.97	-0.40	0.00	-0.32
ΔRIX	-0.50	0.68	-0.32	0.00

In Appendix A additional plots of between several factors summarized are presented for comparison with the correlations calculated.

3.3.2. Pre-Expansion AEP and Wake Losses

The wind farm layout is modeled as it was before the expansion/addition of the 2.0 MW turbines.

The difference in wake losses and production at each turbine site are plotted in Figure 9.

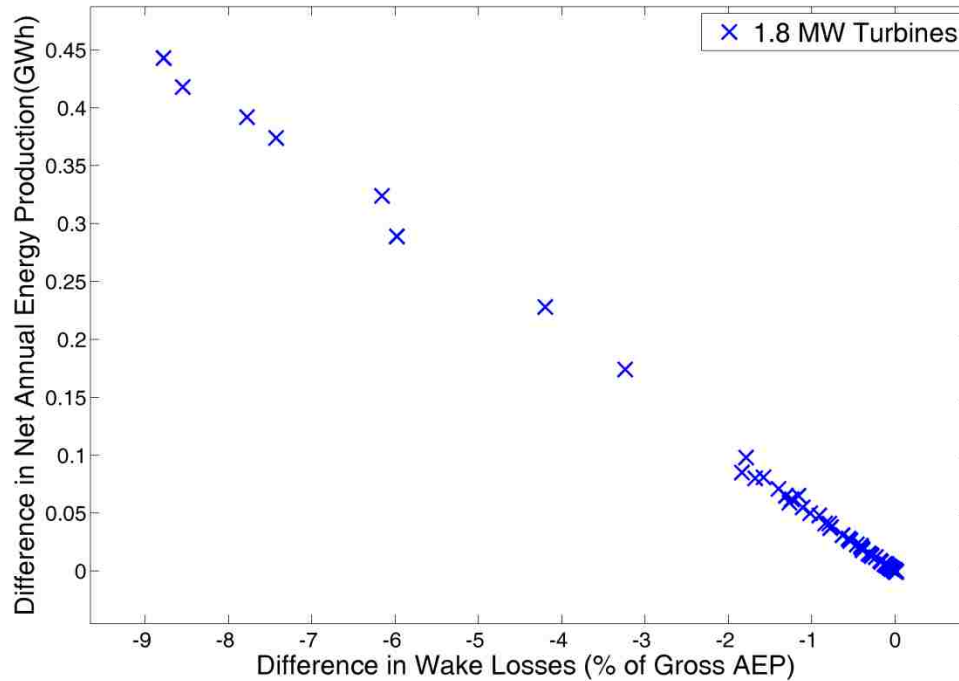


Figure 9 - Difference in production and wake losses for all 1.8 MW turbines. Wake loss difference is found by subtracting results from Pre-expansion analysis from WASP Predictions with no user corrections.

Table 7 - Predictions for Pre-expansion analysis in WASP.

Net AEP (GWh)	Average AEP per turbine (GWh)	Wake Losses (%)	Deviation from measured production (%)	Average Δ RIX (%)
610.070	4.804	8.03	-4.01	4.06

The expansion of the wind farm resulted in an expected increase of the predicted wake losses at several sites. The total of decrease in annual production is **3.962 GWh**.

3.3.3. Empirical User Corrections

It is assumed that the rugged terrain causes overestimations of wind speed due to flow separation induced by steep elevation changes. The empirical user applied alterations which were derived by Mortensen et al (2006), are applied to the wind speed at hub height, for each turbine. It will be assumed that the separation of the flow can both over- and underestimate the wind speed predictions at the turbine sites. When it is assumed that WAsP is overestimating wind speed, the correction will decrease the predicted wind speeds and the opposite for when underestimation is assumed.

3.3.3.1. *Overestimation of Wind Speeds due to roughness of terrain*

The empirical corrections derived from Δ RIX and applied to the wind speeds predictions at each turbine site. The overall predictions are shown in Figure 10 and summary of the predictions is in Table 8.

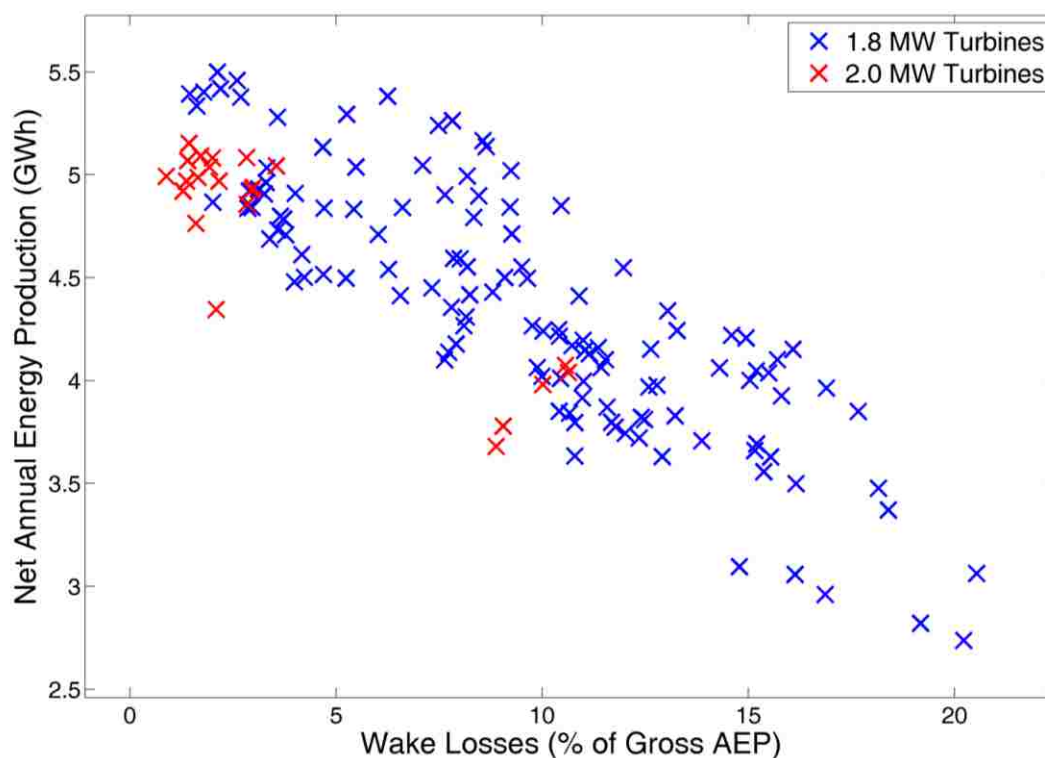


Figure 10 – Predicted Net AEP (GWh) and Wake Losses (%) for all sites in wind farm with empirical correction applied for overestimation.

Table 8 - Predictions from WAsP with empirical correction applied for overestimation.

	Net AEP (GWh)	Average AEP per turbine (GWh)	Wake Losses (%)	Deviation from measured production (%)	Average Δ RIX (%)
For 1.8 MW Turbines	552.778	4.353	9.22	-13.03	4.06
For 2.0 MW Turbines	103.777	4.717	3.62	6.51	5.72
For All turbines	656.555	4.406	8.38	-10.43	4.30

In order to determine which factors within the model affect the production estimates, the correlation between several factors are summarized in Table 9 to Table 11.

Table 9 - Correlation between different factors in WAsP for all turbines with empirical correction applied for overestimation.

	Net AEP	Wake Losses	Elevation	Δ RIX
Net AEP	0.00	-0.85	0.44	-0.62
Wake Losses	-0.85	0.00	-0.30	0.45
Elevation	0.44	-0.30	0.00	-0.42
ΔRIX	-0.62	0.45	-0.42	0.00

Table 10- Correlation between different factors in WAsP for all 1.8 MW turbines with empirical correction applied for overestimation.

	Net AEP	Wake Losses	Elevation	Δ RIX
Net AEP	0.00	-0.85	0.37	-0.68
Wake Losses	-0.85	0.00	-0.65	0.60
Elevation	0.37	-0.65	0.00	-0.60
ΔRIX	-0.68	0.60	-0.60	0.00

Table 11 - Correlation between different factors in WAsP for all 2.0 MW turbines, with empirical correction applied for overestimation.

	Net AEP	Wake Losses	Elevation	Δ RIX
Net AEP	0.00	-0.90	0.81	-0.80
Wake Losses	-0.90	0.00	-0.75	0.69
Elevation	0.81	-0.75	0.00	-0.32
ΔRIX	-0.80	0.69	-0.32	0.00

3.3.3.2. Underestimation of Wind Speeds due to roughness of terrain

The empirical corrections derived from Δ RIX and applied to the wind speeds predictions at each turbine site. The results for all turbine sites are shown in Figure 11 and Table 12.

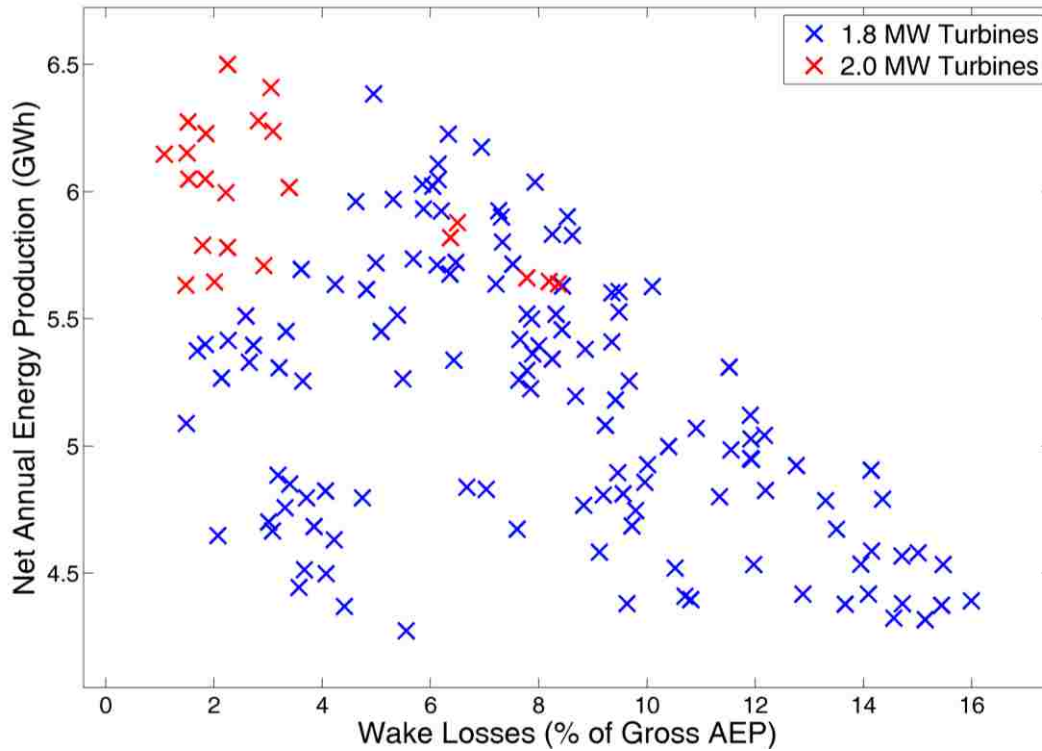


Figure 11 - Predicted Net AEP (GWh) and Wake Losses (%) for all turbine sites, with empirical correction applied for underestimations.

Table 12 - Predictions from WAsP with empirical correction applied for underestimations.

	Net AEP (GWh)	Average AEP per turbine (GWh)	Wake Losses (%)	Deviation from measured production (%)	Average Δ RIX (%)
For 1.8 MW Turbines	654.951	5.157	8.04	3.05	4.06
For 2.0 MW Turbines	131.533	5.979	3.36	35.00	5.72
For All turbines	786.484	5.278	7.29	7.30	4.30

In order to determine what factors within the model affect the production estimates, the correlations between several factors are summarized in Table 13 to Table 15.

Table 13 - Correlation between different factors in WASP for all turbines, with empirical correction applied for underestimations.

	Net AEP	Wake Losses	Elevation	Δ RIX
Net AEP	0.00	-0.53	-0.01	0.48
Wake Losses	-0.53	0.00	-0.19	0.28
Elevation	-0.01	-0.19	0.00	-0.42
Δ RIX	0.48	0.28	-0.42	0.00

Table 14- Correlation between different factors in WASP for all 1.8 MW turbines, with empirical correction applied for underestimations.

	Net AEP	Wake Losses	Elevation	Δ RIX
Net AEP	0.00	-0.40	-0.34	0.46
Wake Losses	-0.40	0.00	0.06	0.40
Elevation	-0.34	0.06	0.00	-0.60
Δ RIX	0.46	0.40	-0.60	0.00

Table 15 - Correlation between different factors in WASP for all 2.0 MW turbines, with empirical correction applied for underestimations.

	Net AEP	Wake Losses	Elevation	Δ RIX
Net AEP	0.00	-0.48	0.88	0.10
Wake Losses	-0.48	0.00	0.02	0.67
Elevation	0.88	0.02	0.00	-0.32
Δ RIX	0.10	0.67	-0.32	0.00

3.4. Wind Resource Grid

A useful feature in WAsP is the wind resource grid displayed as a map over a selected area. This can be used to locate potentially high AEP locations. The map for the wind farm AEP is shown in Figure 12.

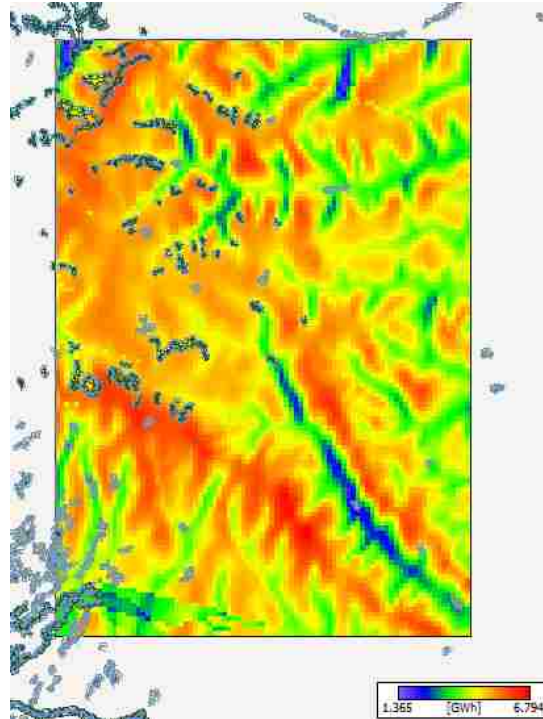


Figure 12 - Resource Grid Map in WAsP showing the potential annual AEP for a 2.0 MW Vestas V80 Turbine within the wind farm boundary.

Figure 12 was used to locate high AEP sites for 6 turbines in the wind farm. The 6 turbines sites chosen all have a low predicted AEP and limited wake losses. Figure 13 has highlighted sites these sites. The turbines were relocated to sites at reasonable distance from other turbines clusters and spaced reasonably from each other to minimize wake losses. Results from the relocation, both changes in wake losses and AEP are plotted in Figure 14.

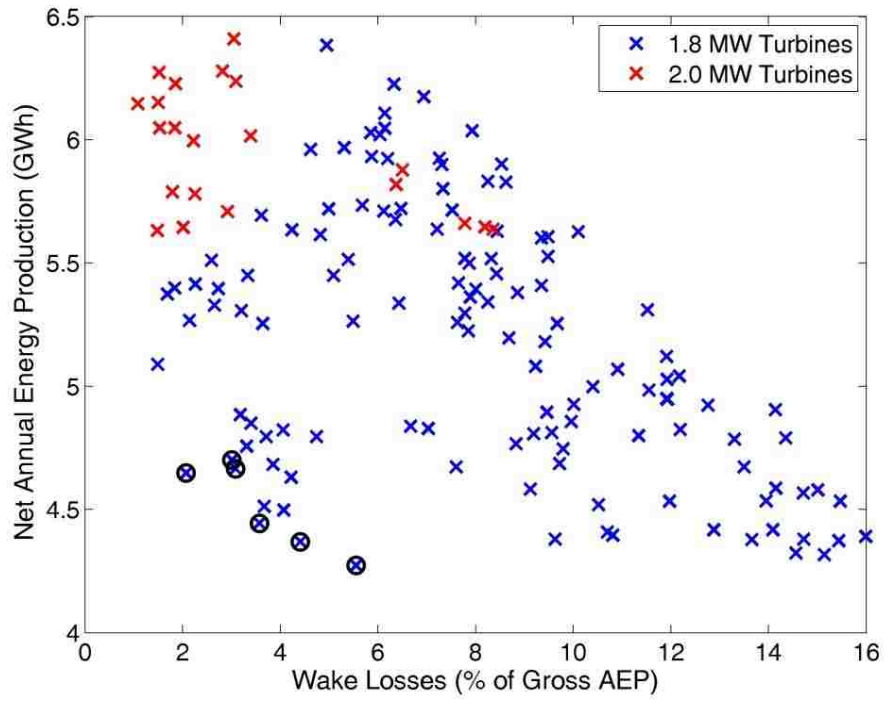


Figure 13 - Predicted Net AEP (GWh) and Wake Losses (%) for all turbine sites. Conditions from case 4 are used and 6 turbines that are relocated are circled (black).

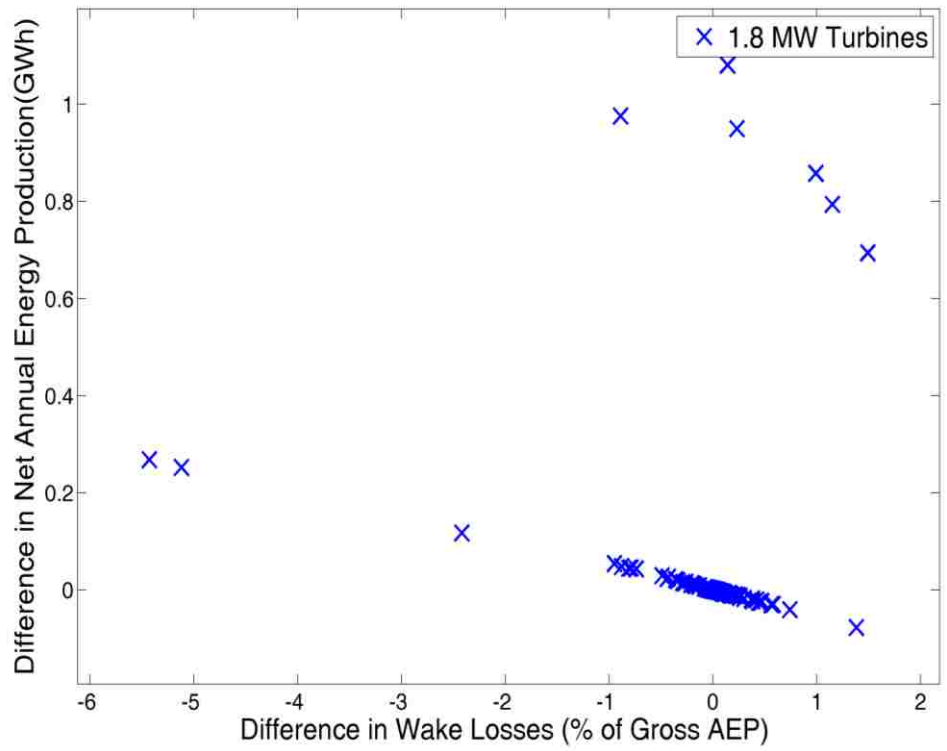


Figure 14 - Changes in wake losses and AEP for all turbines due to the relocation of 6 turbines (Circled in black).

The gain in AEP is **5.943 GWh** with the relocation of the 6 turbines, **5.350 GWh** comes directly from the 6 turbines and the remainder from reduced wake effects.

3.5. Measured Production vs. Predicted Production

Since only data for a single month (January) was available, the predicted AEP was scaled down by a factor determined by the relation of the measured production for which the MET data was available, to measured annual production. The deviation of the scaled predicted power production from the measured power production was also calculated.

3.5.1. Filtering the Measured Production

The measured data is filtered using comparisons and several features of WASP. The wind turbines can be offline due to several reasons. Extensive periods of non-production will skew the analysis and are therefore not used. The problematic turbines are derived by comparing measured production with the fraction of time available. The turbine site with the highest production time is used as the denominator for production time comparisons. If turbines have significantly lower turbine availability than neighboring sites, with similar topographical conditions, then this data is filtered from the analysis. Using the user interface of WASP projections in Google Earth were displayed to locate obstacles not accounted for in the model. This was the instance in one case where a building was effecting the production of 2 turbines. Overall data from 5 turbines was filtered from the analysis.

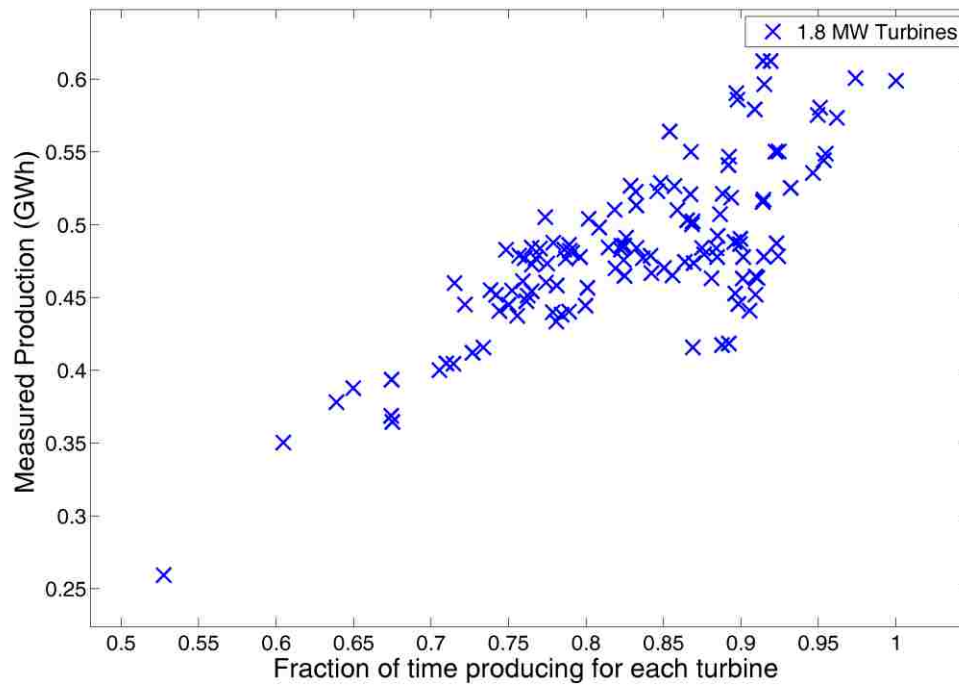


Figure 15 - Fraction of time available and Measured Power Production (GWh) for each turbine site.

3.5.2. WAsP Predictions

The correlation between Predicted and Measured Production is plotted in Figure 16 and calculated in Table 16.

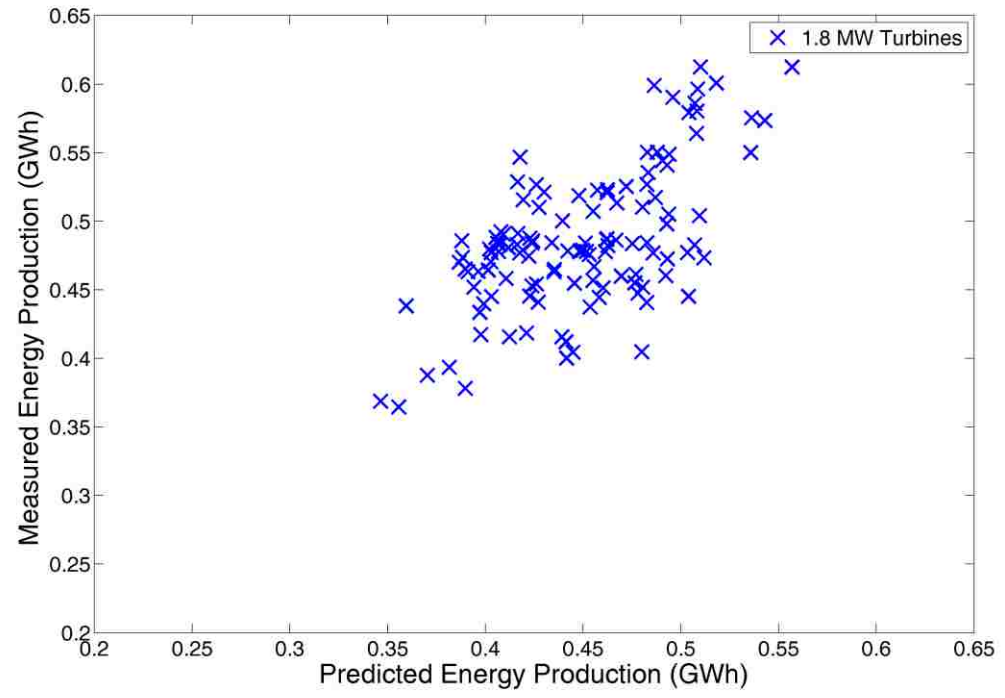


Figure 16 - Scaled Predicted Production (GWh) and Measured Production (GWh) for all 1.8 MW sites.

Table 16 - Correlation Results for Measured Production.

	Scaled AEP	Elevation	RIX
Measured Power Production	0.63	0.53	-0.45

Table 17 - Correlation of Deviation.

	Elevation	ΔRIX	Distance from MET station
Deviation of Scaled Projected Production from Measured Production	0.64	0.38	-0.19

Figure 17 shows the predicted and measured production for each turbine site in the wind farm. The deviation of predicted from measured production is then calculated and plotted in Figure 18.

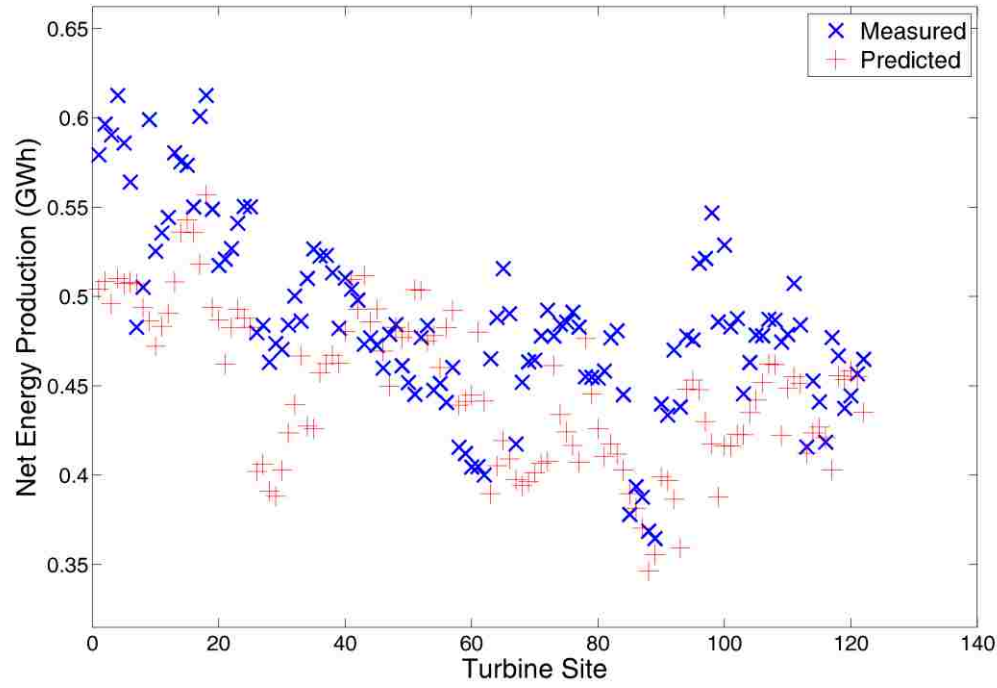


Figure 17 - Scaled Predicted- and Measured Production for all 1.8 MW turbine sites.

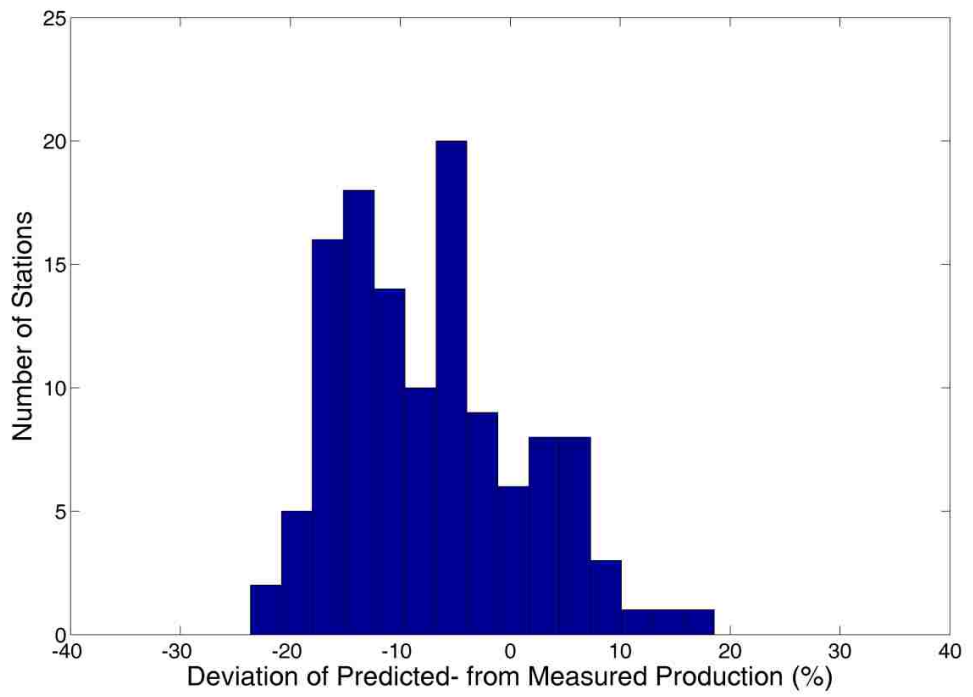


Figure 18 – Histogram of the Deviation (%) of Scaled Predicted Production and Measured Production for all 1.8 MW Turbine Sites.

3.5.2.1. Overestimation of Wind Speeds due to roughness of terrain

The correlation between Predicted and Measured Production is plotted in Figure 19 and calculated in Table 18. The same user corrections for applied overestimations of wind speeds due to terrain roughness are applied at each turbine site.

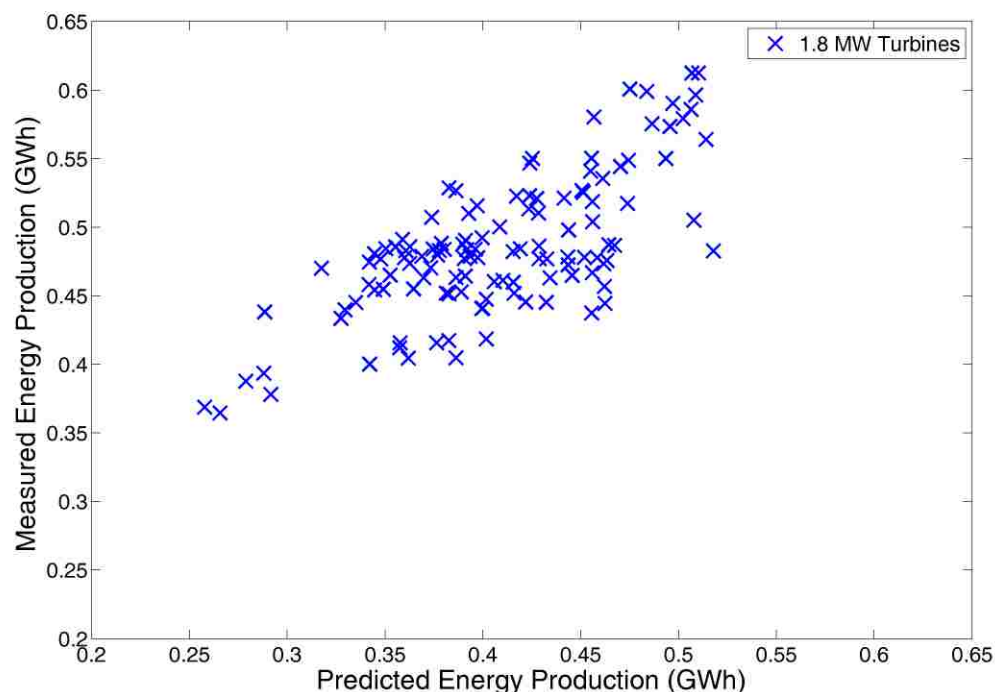


Figure 19 - Scaled Projected Production (GWh) and Measured Production (GWh) for all 1.8 MW sites, for one month. With empirical correction applied for overestimations.

Table 18 - Correlation Results for Measured Production. With empirical correction applied for overestimations.

	Scaled AEP	Elevation	RIX
Measured Power Production	0.73	0.53	-0.45

Figure 20 shows the projected and measured production for each turbine site in the wind farm. The histogram of deviations of projected from measured production is then calculated and plotted in Figure 21.

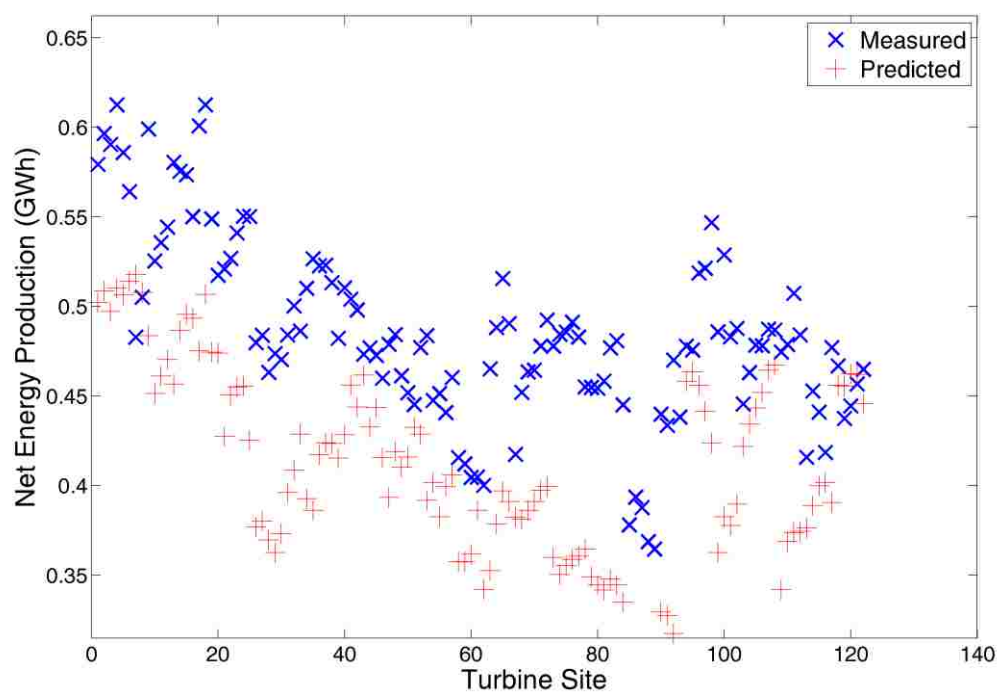


Figure 20 - Scaled Predicted- and Measured Production for all 1.8 MW turbine sites. With empirical correction applied for overestimations.

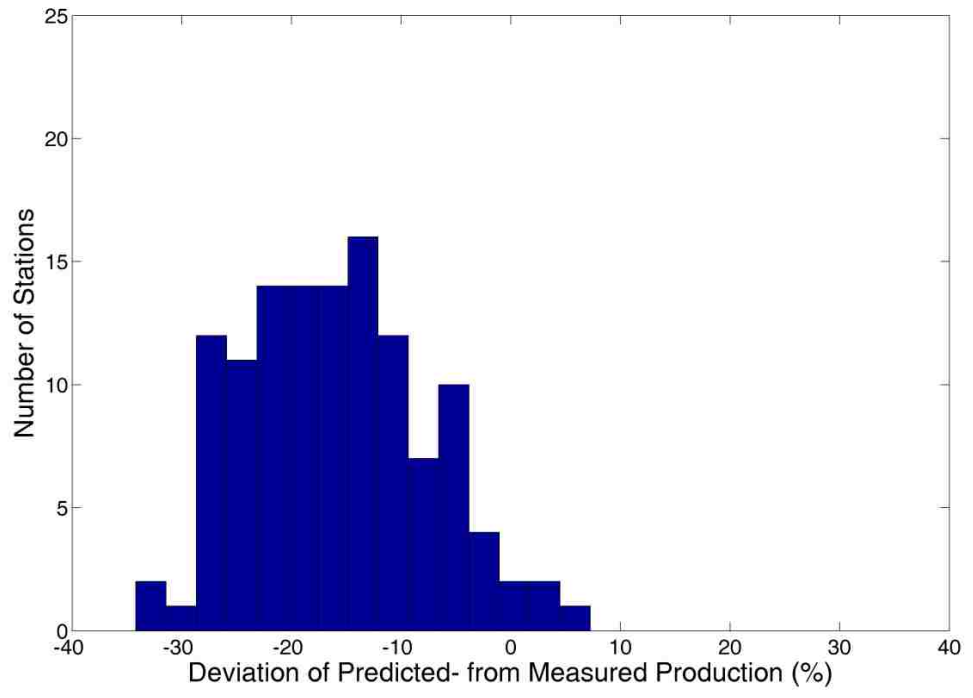


Figure 21 - Histogram of the Deviation (%) of Scaled Predicted Production and Measured Production for all 1.8 MW Turbine Sites. With empirical correction applied for underestimations.

3.5.2.2. *Underestimation of Wind Speeds due to roughness of terrain*

The correlation between Predicted and Measured Production is plotted in Figure 22 and calculated in Figure 23 shows the projected and measured production for each turbine site in the wind farm. The histogram of deviations of projected from measured production is then calculated and plotted in Figure 24.

Table 19. The same user corrections for applied overestimations of wind speeds due to terrain roughness are applied at each turbine site.

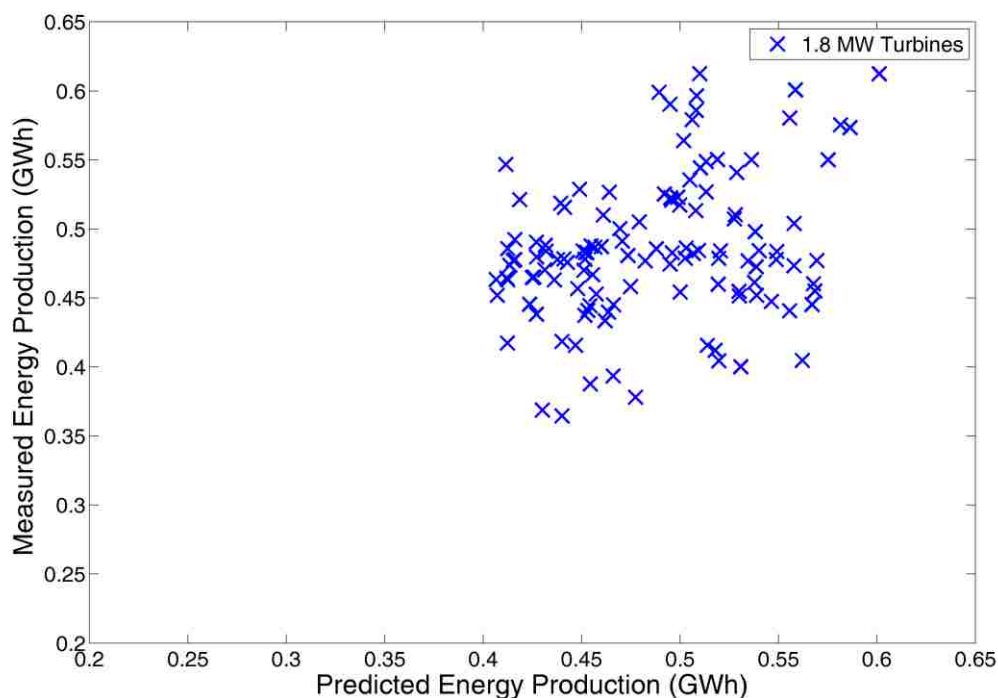


Figure 22- Scaled Predicted Production (GWh) and Measured Production (GWh) for all 1.8 MW sites, for one month. With empirical correction applied for underestimations.

Figure 23 shows the projected and measured production for each turbine site in the wind farm. The histogram of deviations of projected from measured production is then calculated and plotted in Figure 24.

Table 19 - Correlation Results for Measured Production. With empirical correction applied for underestimations.

	Scaled AEP	Elevation	RIX
Measured Power Production	0.29	0.53	-0.45

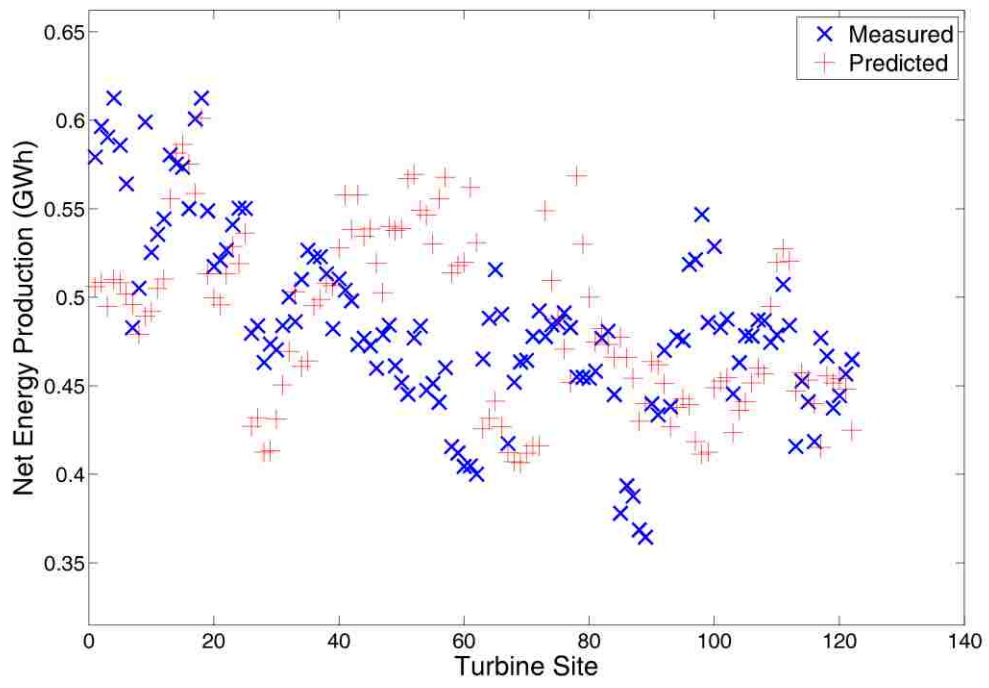


Figure 23 - Scaled Projected- and Measured Production for all 1.8 MW turbine sites. With empirical correction applied for underestimations.

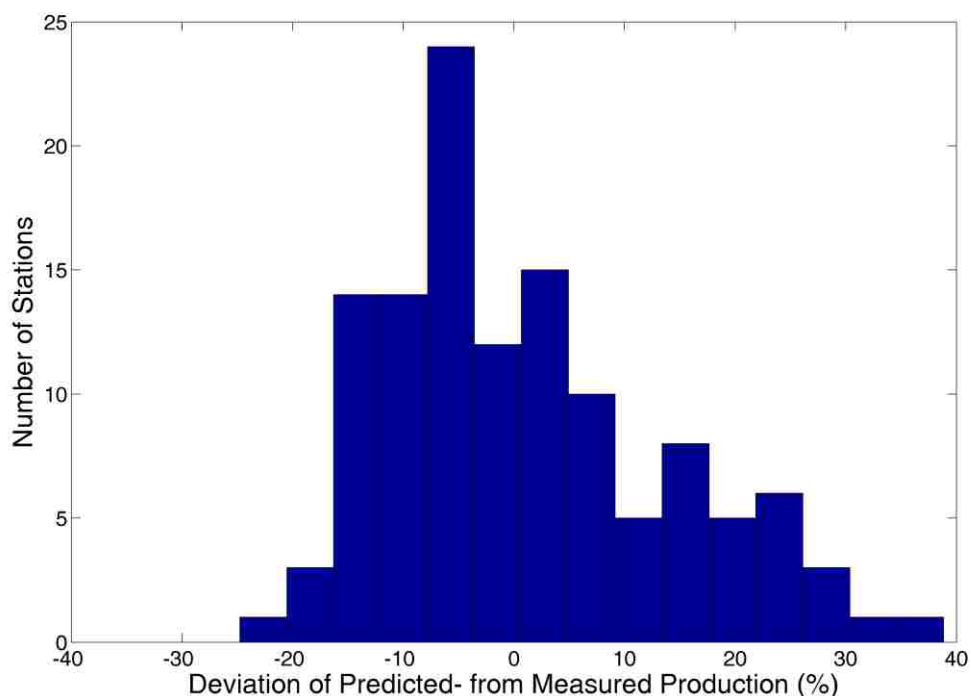


Figure 24 – Histogram of the Deviation (%) of Scaled Projected Production and Measured Production for all 1.8 MW Turbine Sites. With empirical correction applied for underestimations.

3.5.3. Visual Comparison of Ruggedness Index

In order to understand the limitations of WAsP better, the turbine sites are separated into three categories, depending on the severity of the deviation of projected- from measured production. The RIX is calculated in all directions from each grid cell in WAsP. WAsP averages the RIX from all these calculations over all directions, which it returns as an output. In this analysis, only the RIX in the prevailing wind direction and 30 degrees to either side will be mapped and are shown in Figure 26 to Figure 28. The surface roughness polygons will also be plotted on the grid maps.

In addition to this, the 2.0 MW turbine sites are mapped only in the prevailing wind direction with the ruggedness index for the same direction (Figure 25).

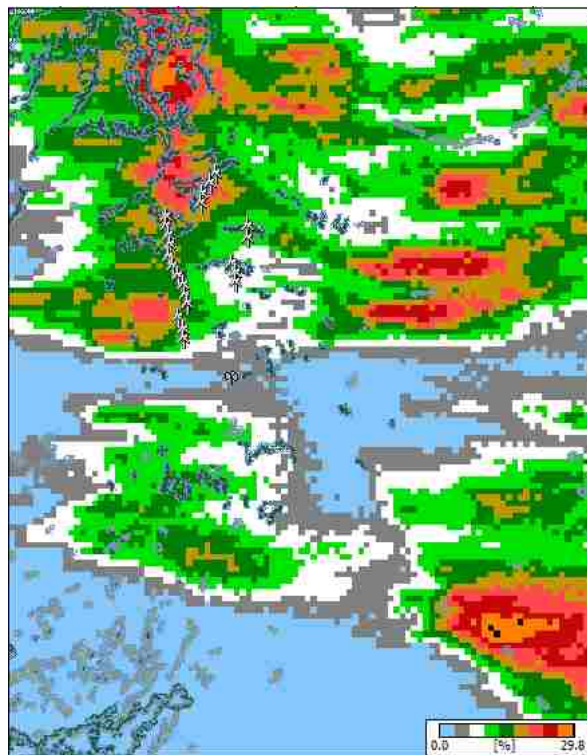
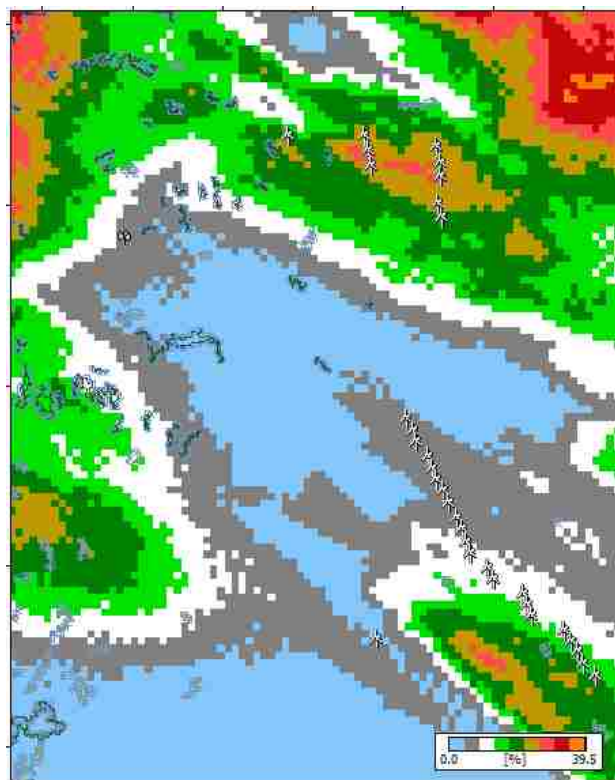
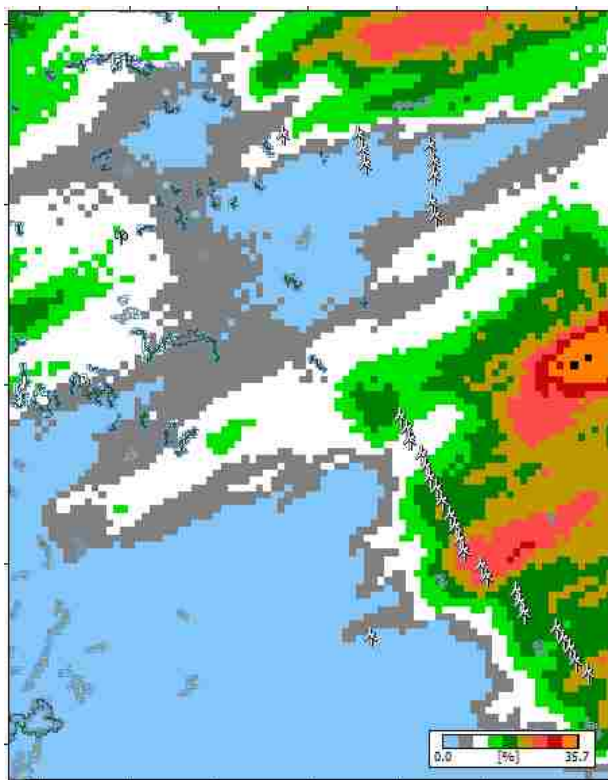


Figure 25 - 2.0 MW Turbine sites mapped with RIX and surface roughness polygons. Figure shows grid map of prevailing wind direction.



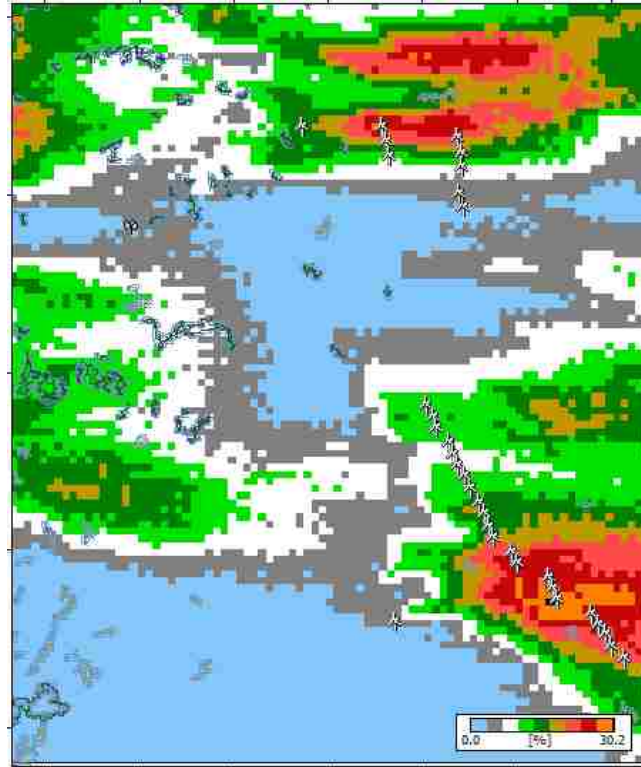
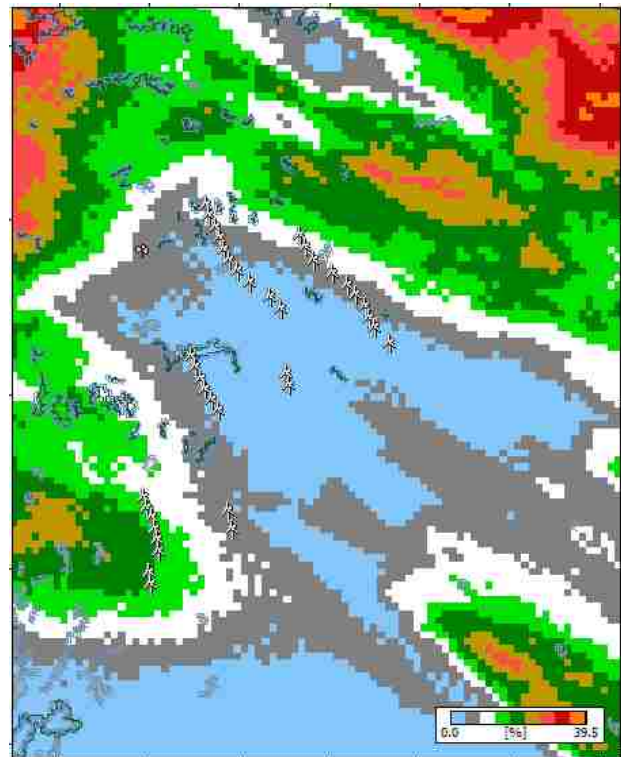
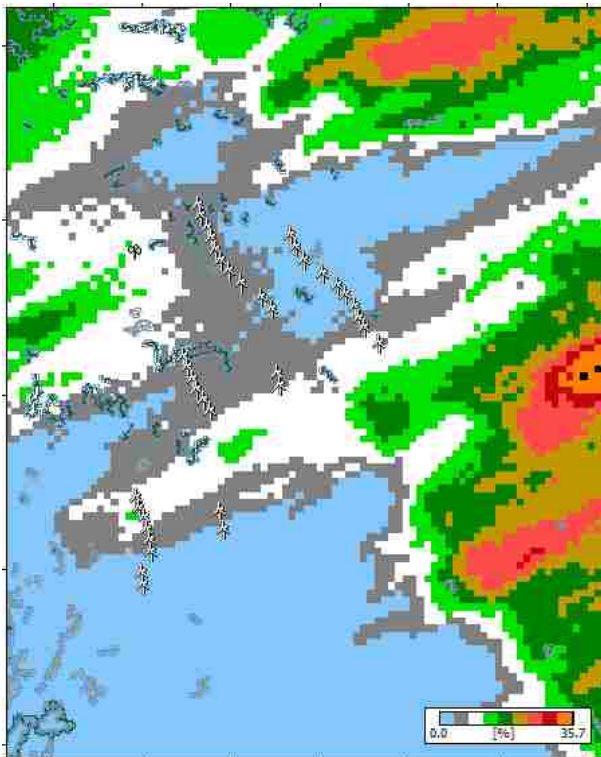


Figure 26- Turbine sites where WASP overestimates production by 10% and over, mapped with RIX grid and surface roughness polygons. Figure shows grid maps of prevailing wind direction (bottom) and wind directions for sections 30° to either side (Top).



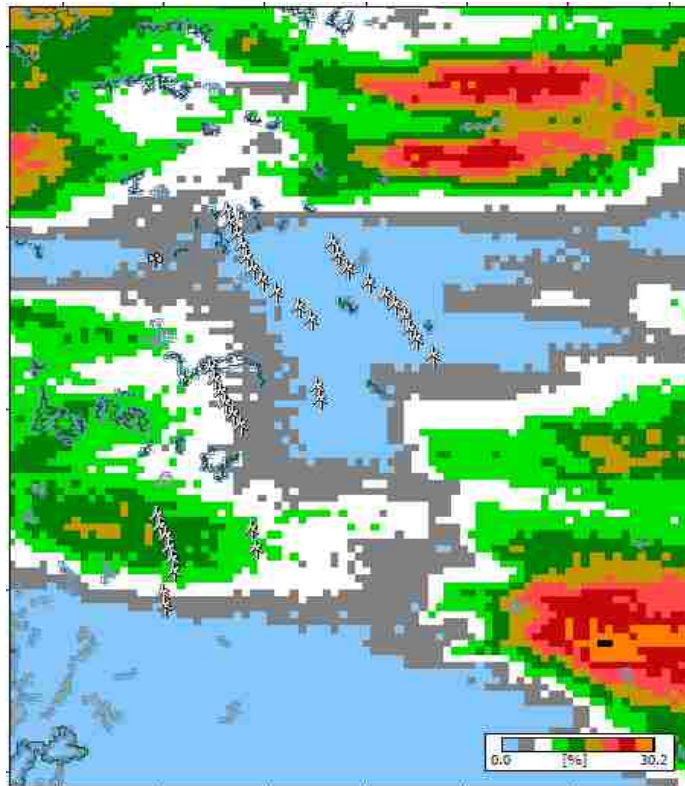
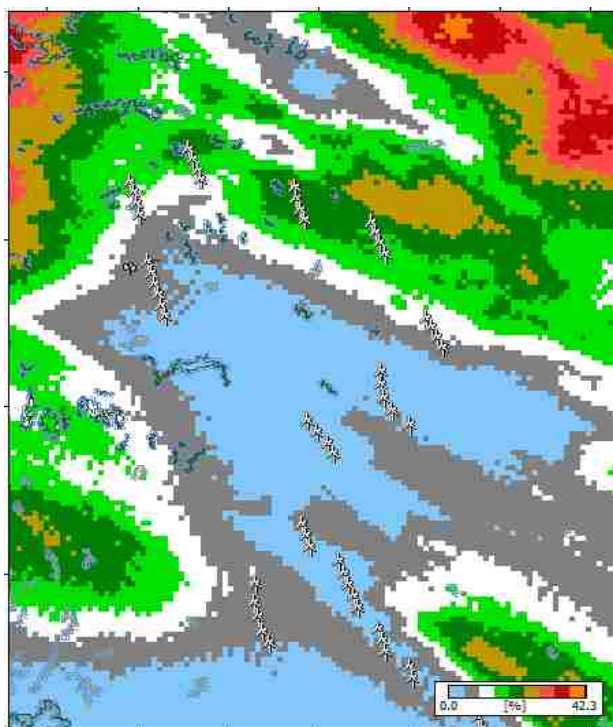


Figure 27 - Turbine sites where WASP underestimates production by 10% and over, mapped with RIX grid and surface roughness polygons. Figure shows maps of prevailing wind direction (bottom) and wind directions for section 30° to either side (Top).



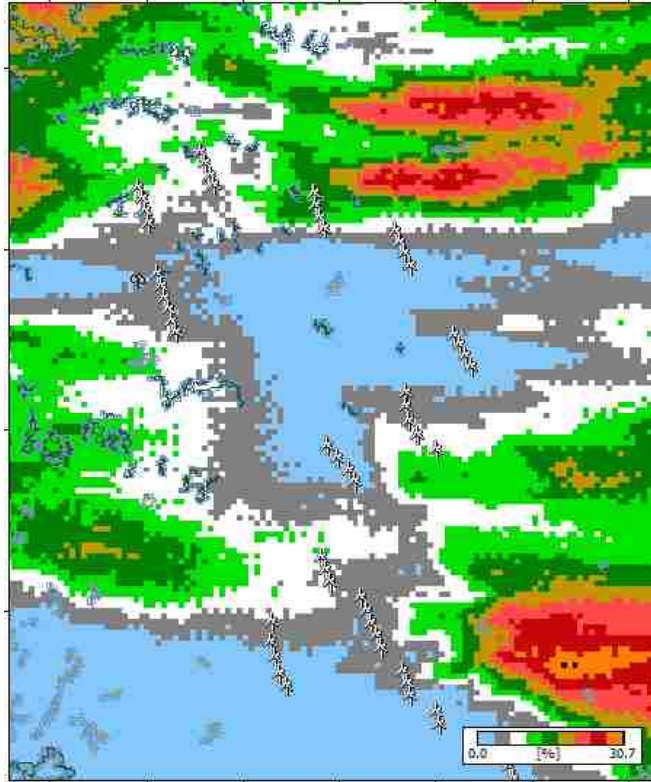


Figure 28 - Turbine sites where WAsP under/over- estimates production by less than 10%, mapped with RIX grid and surface roughness polygons. Figure shows maps of prevailing wind direction (bottom) and wind directions for section 30° to either side (Top).

4. Discussion

4.1. Topographical Data Input

The topographical data was overall satisfactory. The elevation data was of sufficient scale and allowed the model to account for sudden elevation changes, within its operational envelope. The roughness lengths polygons were only available in 30 m scale. In order to account for the changes more accurately, a model of 10 m or less should be used. This would allow for better modeling of the wind farm, for a more detailed analysis. The surface roughness length polygons can be assigned by the user and drawn from Google earth. Having similar spatial scales of orographical data inputs is ideal and would be recommended for future analysis. It is important

to note that some overestimations were noted near dense forest areas. This is a known problem within WAsP, as was noted in Dellwik et al, 2006. These overestimations could be contributing to the 2.0 MW turbine predictions, although comparison with measured data is required for confirmation. If WAsP is used to estimate the production near forest sites, the user must be aware of the skewed projections and account for them.

The RIX values are also high at several locations within the wind farm layout. This can be problematic for the WAsP flow model and user corrections might be necessary.

The predictions of two turbines were overestimated due to the building being excluded from the data input. This resulted in fewer data points for analysis, as the predictions were filtered out of the analysis. For future analysis it is important to include all buildings within the wind farm layout, this will yield a more accurate representation of the wind farm production.

4.2. Meteorological Data

The MET data available from the wind farm, is undeniably the single most important factor in this analysis. Outside the production values, all other data used in this thesis is available to the public. Although MET data is available at a location in close proximity to the wind farm, the complexity of the terrain and the use of macro scale models, do not yield sufficient accuracy for wind farm analysis (Hermannsson, 2012).

The observed wind climate analysis of the MET data (seen in Figure 7) seems to alter the MET data insignificantly when compared to a simple wind rose of the yearly MET data as seen in Figure 29.

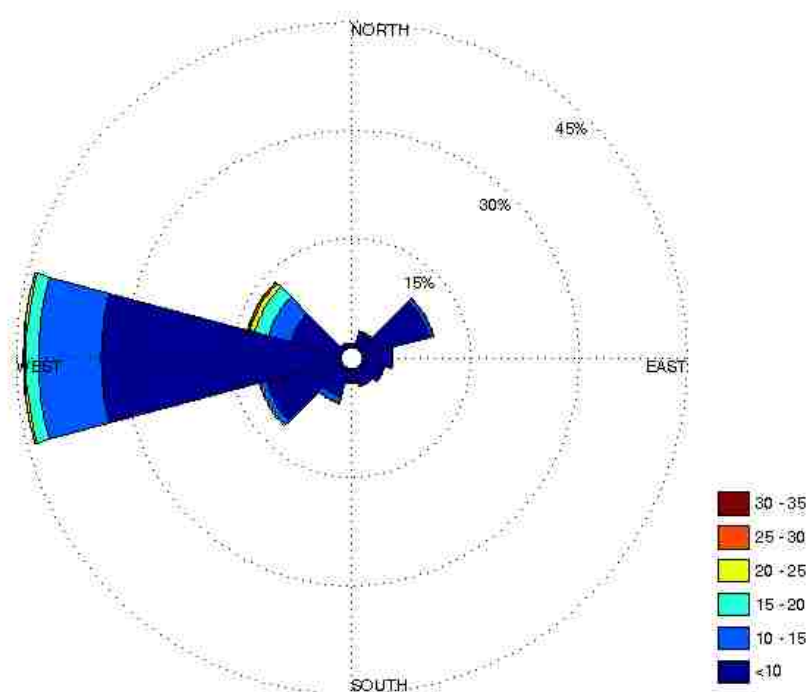


Figure 29 - Wind Rose plotted from the yearly MET Data.

Although WAsP recommends using as several years of MET data as a basis for predictions, the data available is sufficient for comparisons of measured production. However, using the program for long term predictions will require more years of data.

4.3. Net Annual Power Production

4.3.1. WAsP AEP Predictions

WAsP compares favorably without any user alterations being applied. Table 3 suggests that WAsP slightly underestimates the production of the entire wind farm and for the 1.8 MW turbine sites. The net AEP predictions for the 2.0 MW turbines show significant overestimations when compared to the measured AEP. However, the measured average AEP for the 2.0 MW turbines from The wind speed is predicted at hub height for each turbine site and the power production

can then be estimated. The predictions for all turbines will be presented and separate results for 1.8MW and 2.0MW turbine sites. The results shown are a summary for all wind directions.

The measured AEP from the wind farm is summarized in **Error! Not a valid bookmark self-reference.**. It includes the availability of turbines and average AEP per turbine.

Table 2 is lower than the AEP for the 1.8 MW turbines. This is an anomaly which could be either due to the terrain or the turbines are simply not producing. This makes it difficult to assess the overall accuracy of predictions for the 2.0 MW turbines. However, it will be assumed that WASP is over predicting the AEP, due to both the proximity to the forest boundaries and ruggedness of terrain. Table 4 shows that the net AEP has strong correlation with wake losses, which was expected as wake losses contribute directly to the calculation of net AEP. The net AEP shows very little correlation with both elevation and RIX of the terrain. The low correlation with elevation is surprising, however the layout of the wind farm is a big contributor to the predictions and might lower the effects of elevation on production.

Figure 8 indicates that several turbines are located in areas where predicted wind speed is lower than desirable which cannot be contributed to high wake losses. Six of these turbines were relocated to improve their production with the help of WASP.

4.3.2. Empirical User Corrections

4.3.2.1. Overestimation of Wind Speeds due to roughness of terrain

After applying the WASP recommended user corrections to each of the turbine sites, the net AEP decreased as was expected. Table 8 shows that the corrections increase the accuracy of the 2.0 MW turbines, but it lowers the accuracy of the overall AEP predictions. The measured AEP of the 2.0 MW turbine sites is lower than expected and it cannot be ruled out that the WASP

predictions (with no user corrections) are accurate. The correlation of AEP with ΔRIX increases, this was expected as AEP is now a function of ΔRIX when user corrections are applied.

4.3.2.2. Underestimation of Wind Speeds due to roughness of terrain

The overall results were as expected, the net AEP increased due to the applied user corrections. Table 12 shows that for the 1.8 MW turbines, the predictions are more accurate than when no corrections are applied. All predictions do not account for turbine availability, which would increase the accuracy of these predictions. The wind speed is predicted at hub height for each turbine site and the power production can then be estimated. The predictions for all turbines will be presented and separate results for 1.8MW and 2.0MW turbine sites. The results shown are a summary for all wind directions.

The measured AEP from the wind farm is summarized in **Error! Not a valid bookmark self-reference.** It includes the availability of turbines and average AEP per turbine.

Table 2 shows the availability around 98% and so the net AEP predictions for the 1.8 MW turbines would be extremely accurate. However, the overall accuracy is lower due to the overestimations at the 2.0 MW turbine sites. These overestimations are significant and the uncertainty with the measured data makes it difficult to recommend applying these user corrections to the entire wind farm.

4.3.3. Pre-Expansion AEP and Wake Losses

This analysis was included to highlight the useful features of WAsP. It was always known that there would be an increase in wake losses as Figure 9 clearly shows. The magnitude of wake losses is less than expected as the 2.0 MW turbines were placed directly in the prevailing wind

direction when the wind farm was expanded. The increase in production clearly outweighs the small loss in production as illustrated in both the projected data and the wind farm net AEP.

4.4. Measured Production vs. Measured Production

The data for the measured 10 minute production of the 1.8 MW turbine sites was only available for a single month and the MET data was only available for half of this month. This makes the analysis of this data very difficult and the downscaling of the annual projections was necessary. The wind speed and direction varies significantly with season and location. If we compare wind rose plots of 2 different sites (Figure 30), they differ from the WAsP projected wind roses and the annual wind rose plot seen in Figure 29. Even with the scaling the comparisons of projected and measured data is statistically inefficient and difficult. The results will only be used to support general observations and trends noticed from the available data.

4.4.1. WAsP Predictions

The correlation between the scaled projections and measured production is less than desired (see Table 16). This was expected as the wind speed and direction effects the power production immensely and the differences between seasons and years can be significant. The calculated Weibull wind speed of the turbine station in the closest proximity to the MET station was 9.00 m/s. The average annual predicted wind speed for all sites is 7.3 m/s (see Figure 7) and 9.66 m/s for the measured data (of the month available). The increased wind speeds measured for the single month, suggest that even with the scaling, the predictions are expected to underestimate the energy production. The histogram plotted in Figure 18 supports that theory as most turbines seem to predict lower energy production than measured. Table 16 suggests that the measured energy production has a higher correlation with elevation. It is difficult to evaluate the effects of

higher correlation without having annual data for all turbines. The directionality of the wind for the month available could explain the higher correlation with elevation. The alternative is that the effects of elevation changes are not picked up by the WAsP model, leading to errors in the predictions. The correlation of measured production and Δ RIX indicates that the terrain is having a larger effect on the production than WAsP estimates. Table 4 shows that the predicted AEP does not show a significant correlation with Δ RIX, this could indicate that WAsP is again not sufficiently accounting for the ruggedness of the terrain in its predictions.

4.4.2. Empirical User Corrections

4.4.2.1. Overestimation of Wind Speeds due to roughness of terrain

The user corrections have improved the correlation of measured production and predicted production (see Table 18). Figure 23 and Figure 24 confirm that the deviation indicates underestimations of production at almost all turbine sites. The underestimations were expected, both due to the aforementioned wind speed differences and user corrections applied. It is hard to identify whether the user corrections improve the accuracy of WAsP with this analysis.

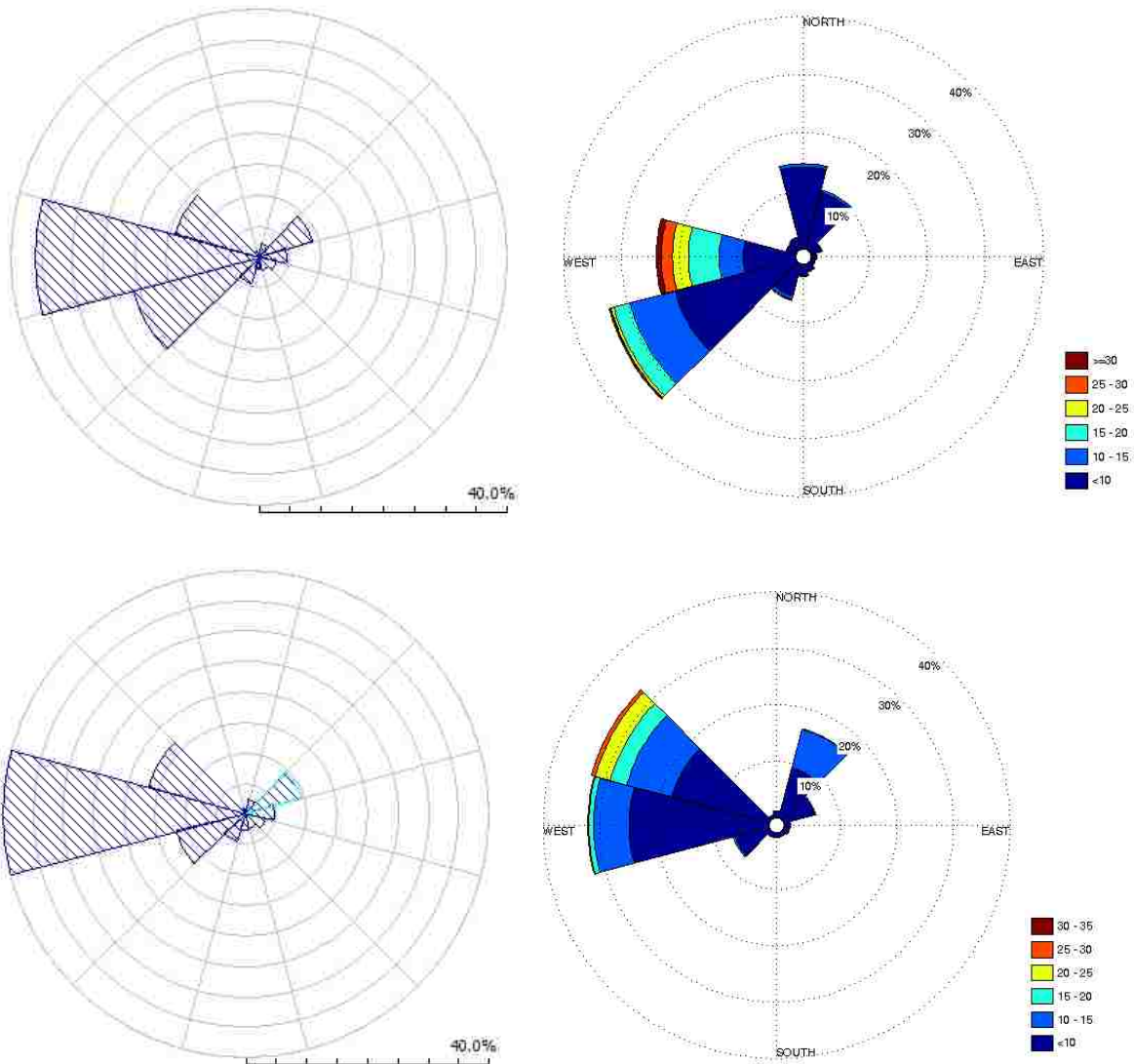


Figure 30 - Wind Roses from WAsP and monthly data, for 2 different turbine sites, distributed in different locations around the wind farm layout.

4.4.2.2. Underestimation of Wind Speeds due to roughness of terrain

The user corrections lowered the correlation between measured and predicted production significantly. Figure 23 shows the projected and measured production for each turbine site in the wind farm. The histogram of deviations of projected from measured production is then calculated and plotted in Figure 24.

Table 19 has the correlation as only 0.29 and Figure 22 shows how the data is scattered. Even though the comparison can be difficult with limited data available, the correlation is lowered than desired. This indicates that the user corrections do not improve the accuracy of WAsP. Figure 23 and Figure 24 indicate that several stations are now overestimating the production. This would seem unlikely as the wind speeds at these stations are significantly higher for the month available than for the annual predicted wind speeds. This suggests that WAsP is not underestimating the wind speeds due to the ruggedness of the terrain.

4.4.3. Visual Comparison

The RIX is calculated by WAsP for all wind directions or sectors. However, WAsP returns the averaged RIX of all directions when the user exports the predicted values from WAsP. The user corrections use the averaged RIX, when deriving the empirical correction factor. Figure 26 shows sites that WAsP overestimates the power production when compared to the one month of data available. Figure 25 shows the averaged RIX with the 2.0 MW turbines sites, where the measured AEP suggests WAsP is over predicting the net AEP. Looking at these figures, the overestimations are clearly at sites in close proximity to areas with high RIX values in the prevailing wind direction or close to it.

Figure 31 shows the entire wind farm layout with the averaged RIX. By looking at this figure, the average RIX would indicate that several other sites would be overestimating the energy production which is not supported by the data. The visual comparisons indicate that a weighted average of RIX, determined by the frequency of wind directions would be a better method for user corrections. Of course this theory would have to be confirmed by analyzing the annual measured production of all sites.

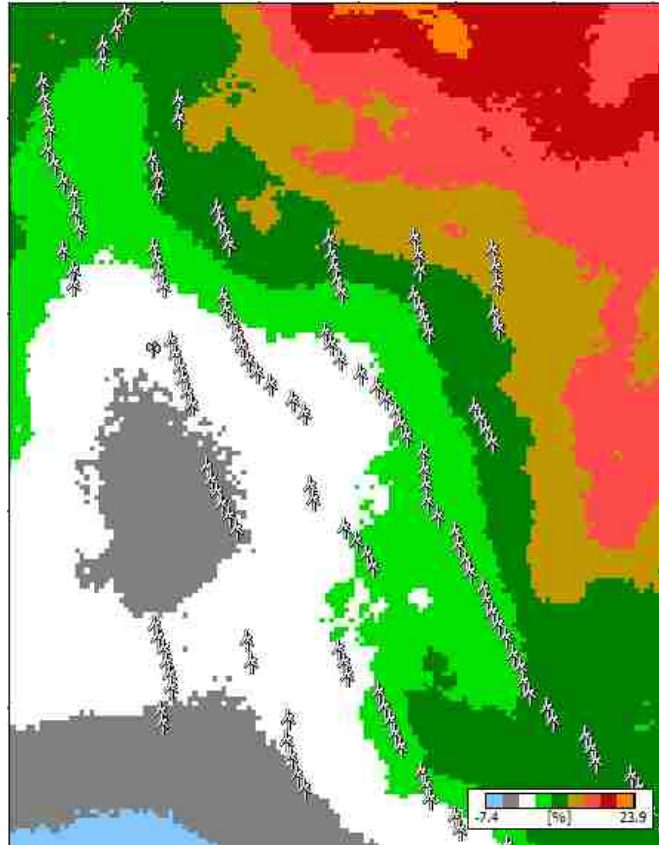


Figure 31 - All Turbine sites mapped with RIX averaged over all directions and surface roughness polygons.

Figure 27 and Figure 28 do not show a clear trend for the cause of deviations of these turbine sites. The culprit could simply be the lack of data available.

4.5. Final Analysis

When all the results are analyzed, the WASP predictions with no user corrections, seems to be the most accurate method for predicting the AEP of the wind farm. When over-estimations are assumed, there is little or no correlation with the measured production for January of the 1.8 MW turbine sites and so it is assumed that WASP does not under-estimate AEP due to the ruggedness of the terrain. The terrain within the wind farm layout is rugged but seems to have very little effects on WASP. At some sites, located in close proximity to highly rugged sites in the

prevailing wind direction, there seems to be some over-estimations. By applying the recommended user corrections for over-estimations, WAsP significantly underestimates the AEP of the wind farm. This indicates the applying them to all sites might not be an accurate method. With the results available, it would be recommended to use the original WAsP predictions with some user corrections due to over-estimation at some sites close the high RIX areas (in the prevailing wind direction). However, in order to confirm the need for user alterations, the annual measured production data for all turbine sites (1.8-and 2.0 MW) will need to be analyzed. This analysis could help determine what sites are possibly problematic for WAsP. The overall accuracy of WAsP is remarkable when the ruggedness of terrain is considered. This is not surprising as other studies have reached the same conclusions (Beaucage, 2012). By using no user corrections, WAsP is able to predict the net AEP with only a small error or – 1.2%. The question mark surrounding the 2.0 MW measured annual production might skew that figure. But, if we assume that the predictions for the 1.8 MW turbine sites are more accurate, then the error is still only -4.7%. This is a remarkably low number if we consider how WAsP estimates the AEP from wind speed predictions. WAsP predicts the wind speed at all sites and combines it with the wind turbine characteristics to calculate the production. The production is related to wind speed in the third power which indicates that WAsP only under-estimates the wind speeds by -1.7%.

5. Conclusions

The usefulness of WAsP as a tool for both site selection and wind farm layout is highlighted by this research. Its performance in complex topographical conditions is impressive and only helps to strengthen its reputation in the wind energy industry. Micro models are the single most important tool to accurately estimate the long term feasibility of wind energy projects, and can be combined with macro models to locate and design an entire wind farm. The macro model is a useful tool to locate a feasible site, whereas installing MET tower and using WAsP can accurately model and site all turbines at a feasible location. As a pre-construction tool, WAsP can be a cost effective tool.

As computer models become increasingly more sophisticated and accurate, the interpretation of those results must not be taken at face value without understanding their significance. Even though WAsP was used to evaluate a rugged terrain that might test the boundaries of its operation envelope, the model performed well in the overall projection of the wind farm. The visual comparisons highlighted some problems with WAsP as they suggest that when a turbine site is at a site in close proximity to either or both forest areas or areas with large ΔRIX values, the user corrections help project a more accurate production and wind speed. It is important to understand the limitations of WAsP, especially in areas of complex topography. These corrections could be improved by using a weighted empirically calculated factor from ΔRIX but more data is needed.

It is recommended that the results from this research be further validated with acquiring several years of data, both MET data and for individual turbines. However even with the limited data and rugged terrain, WAsP performed exceptionally. WAsP is set to further improve its accuracy. In 2013, a new version of WAsP will be released. This version will combine a computation fluid

mechanics model with the current models to improve the predictions in rugged terrain and wake losses within a wind farm. It would be interesting to combine the results highlighted here, with the predictions of the new version of WAsP. It is clear that the wind energy industry has many accurate and useful micro models to choose from and it is also clear that WAsP will continue to be an industry standard for wind farm assessments.

Bibliography

- American Wind Energy Association (AWEA). (2013, January 30). *www.awea.org*. Retrieved January 30, 2013, from American Wind Energy Association: http://www.awea.org/learnabout/industry_stats/index.cfm
- Beaucage, P. (2012). *Wind Flow Model Performance - Do more sophisticated model produce more accurate wind resource estimates?* Albany, NY: AWS Truepower.
- Berge, E., Gravdahl, A., Schelling, J., Tallhaug, L., & Undheim, O. (2006). Wind in complex terrain. A comparison of WAsP and two CFD-models. *In proceedings from EWEC 2006*. Athens: WindSim.
- Bowen, A. J., & Mortensen, N. G. (2004). *WAsP prediction errors due to site orography*. Roskilde, Denmark: Risø National Laboratory.
- Bowen, A., & Mortensen, N. (2006). Exploring the limits of WAsP: the Wind Atlas Analysis and Application Program. *Proceedings of the 1996 European Union Wind Energy Conference, May 20-24*, (pp. 584-587). Goteborg.
- Corbett, J., Ott, S., & Landberg, L. (2007). The new WAsP flow model: a fast, linearized Mixed Spectral - Integration model applicable to complex terrain. *European Wind Energy Conference and Exhibition*.
- Dellwik, E., Landberg, & Jensen, N. O. (2006). WAsP in the Forest. *Wind Energy, Volume 9, Issue 3, May/June*, 211–218.
- Department of Wind Energy, T. U. (2012, February 24). WAsP 10 Help Facility and On-line Documentation. Denmark.
- EIA. (2012, December). *Annual Energy Outlook 2013, Early release review*. Retrieved December 25, 2012, from [http://www.eia.gov/forecasts/aeo/er/pdf/0383er\(2013\).pdf](http://www.eia.gov/forecasts/aeo/er/pdf/0383er(2013).pdf)
- FERC. (2012, December). *Federal Energy Regulatory Commission*. Retrieved February 16, 2013, from <http://www.ferc.gov/legal/staff-reports/dec-2012-energy-infrastructure.pdf>
- FERC. (2013, January). *Federal Energy Regulation Commission*. Retrieved February 17, 2013, from <http://www.ferc.gov/legal/staff-reports/2013/jan-energy-infrastructure.pdf>
- Frank, H. P., Rathmann, O., Mortensen, N. G., & Landberg, L. (2001). *The Numerical Wind Atlas - the KAMM/WAsP Method*. Roskilde, Denmark: Riso.
- Hermannsson, H. (2012). *Assessment of Wind Energy Production Software, Masters Thesis*. Seattle: University of Washington.

- Miljødata, E. o. (2002). *Case studies calculating wind farm production-Main Report*. Denmark: Energi- og Miljødata.
- Mortensen, N. G., Heathfield, D. N., Myllerup, L., Landberg, L., & Rathmann, O. (2007, January). *Getting Started with WAsP 9*. Retrieved December 26, 2013, from WAsP: <http://www.wasp.dk/Products/WAsP.aspx>
- Mortensen, N., Bowen, A. J., & Antoniou, I. (2006). Improving WAsP predictions in (too) complex terrain. *2006 European Wind Energy Conference and Exhibition*. Athens: Riso National Laboratory, University of Canterbury.
- Periera, R., & Guedes, R. S. (2006). Comparing WAsP and CFD wind resource estimates for the "regular" user. *Proceedings from EWEC 2010*. Warsaw: Poland.
- Petersen, E., Mortensen, N. G., Landberg, L., Højstrup, J., & Frank, H. (1997). *Wind Power Meteorology. Risø-I-1206(EN)*. Roskilde: Risø National Laboratory.
- Rathmann, O., Barthelmie, R., & Frandsen, S. (2006). Turbine Wake Model for Wind Resource Software. *European Wind Energy Conference and Exhibition*. Denmark: Risoe National Laboratory.
- Seguro, J., & Lambert, T. (Volume 85, Issue 1, March 2000). Modern estimation of the parameters of the Weibull wind speed distribution for wind energy analysis. *Journal of Wind Engineering and Industrial Aerodynamics*, 75–84.
- Sumner, J., Sibuet Watters, C., & Masson, C. (2010). CFD in wind energy: the virtual, multiscale wind tunnel. *Energies vol 3*, 989-1013.
- Troen, I. (1990). A high resolution spectral model for flow in complex terrain. *Ninth Symposium on Turbulence and Diffusion*, (pp. 417-420). Roskilde.
- Truepower, A. (2010). *openWind - Theoretical basis and validation. Version 1.3*. Albany, NY: AWS Truepower.
- VanLuvanee, D., Rogers, T., Randall, G., Williamson, A., & Miller, T. (2009). Comparison of WAsP, MS-Micro/3, CFD, NWP, and Analytical Methods for Estimating Site-Wide Wind Speeds. *Presentation from AWEA Wind Resource Assessment Workshop*. Minneapolis, MN.
- Vestas. (2005). *V80-1.8 MW, Versatile Megawattage*. Retrieved February 20, 2013, from http://pse.com/inyourcommunity/kittitas/Documents/Vestas_turbine_facts.pdf
- Walford, C. A. (2006). *Wind Turbine Reliability: Understanding and Minimizing Wind Turbine Operation and Maintenance Costs*. Albuquerque, New Mexico: Sandia National Laboratories.

WAsP. (2012, July 26). *WAsP*. Retrieved November 15, 2012, from <http://www.wasp.dk/Products/WAsP.aspx>

WAsP. (2012). WAsP 10.2. *Wind Turbine Generators*. Denmark: Vestas.

Appendix A - Predicted Production

WAsP Predictions

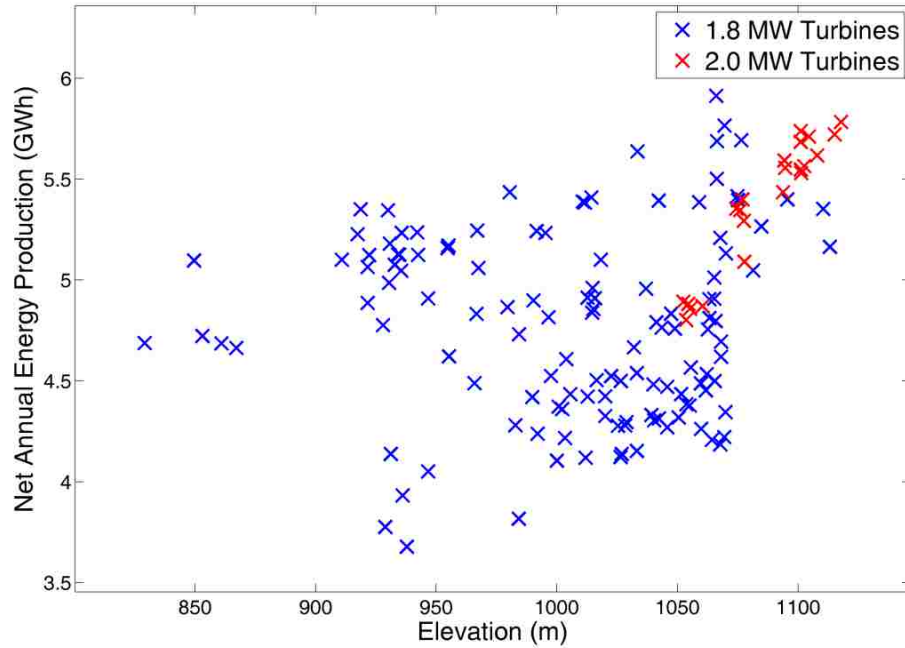


Figure 32 – Net AEP (GWh) with elevation above sea level (m). No user corrections.

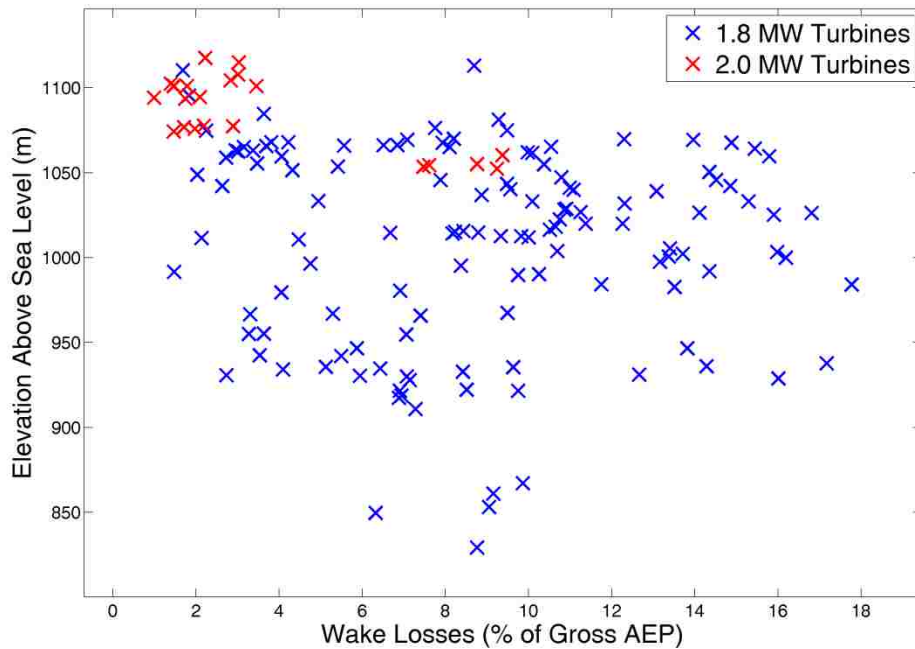


Figure 33 – Wake losses (% of gross AEP) with elevation above sea level (m). No user corrections.

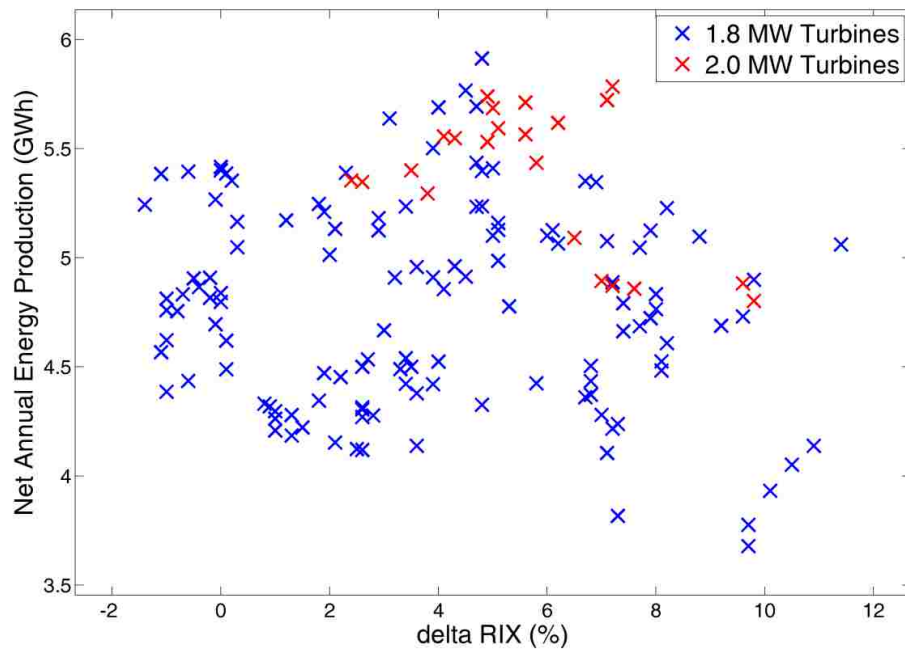


Figure 34 – Net AEP (GWh) with Δ RIX (%).No user corrections.

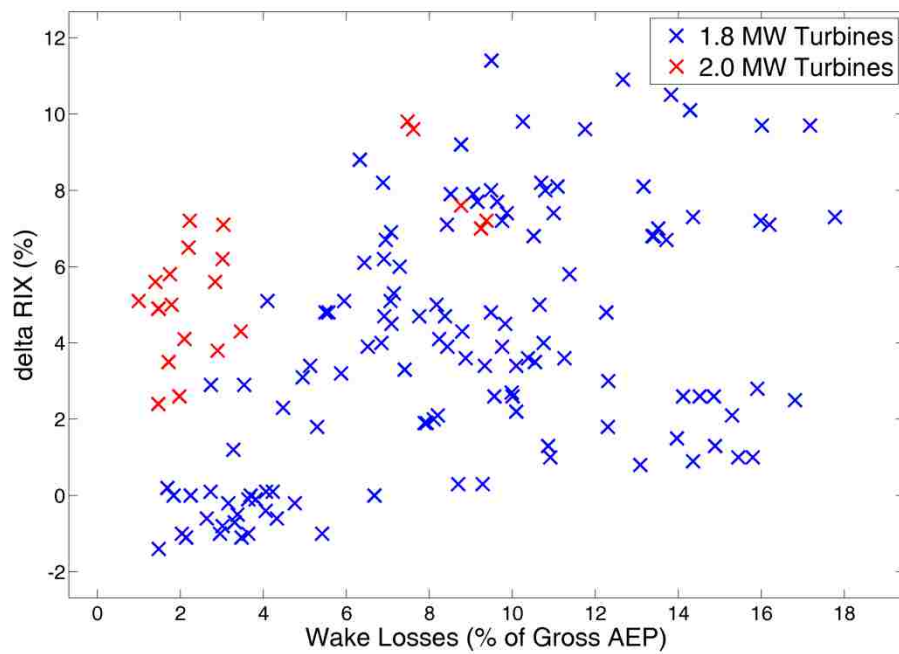


Figure 35 – Wake losses (% of gross AEP) with Δ RIX(%). No user corrections.

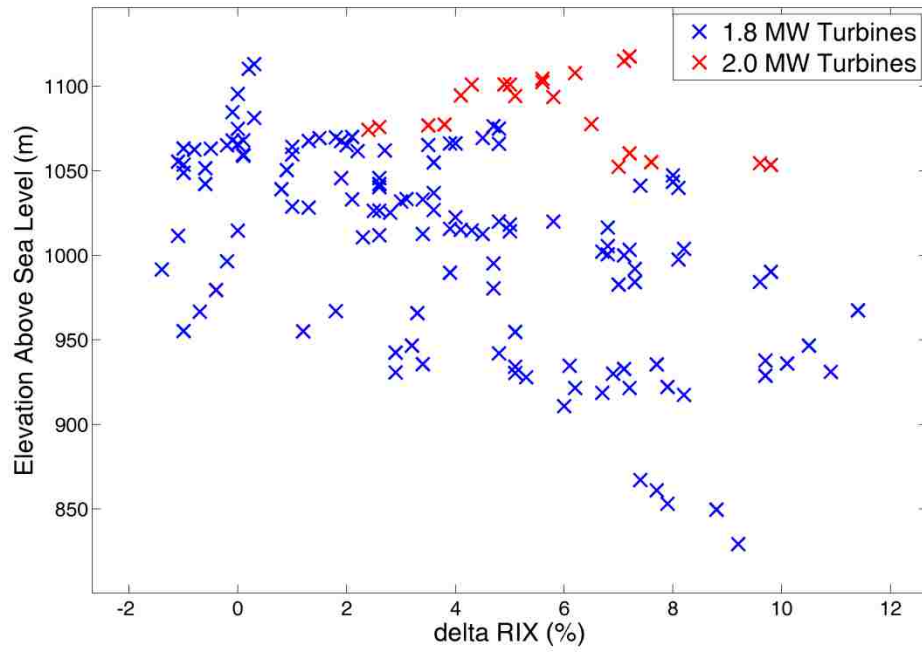


Figure 36 - Δ RIX(%) with elevation above sea level (m). No user corrections.

Overestimation of Wind Speeds due to roughness of terrain

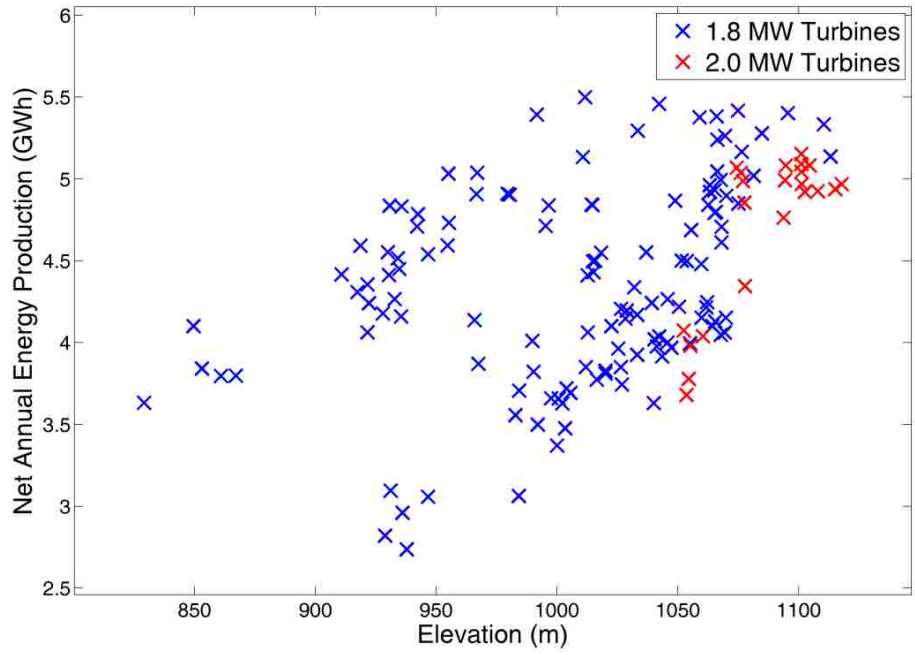


Figure 37 - Net AEP (GWh) with elevation above sea level (m). User correction for overestimations applied.

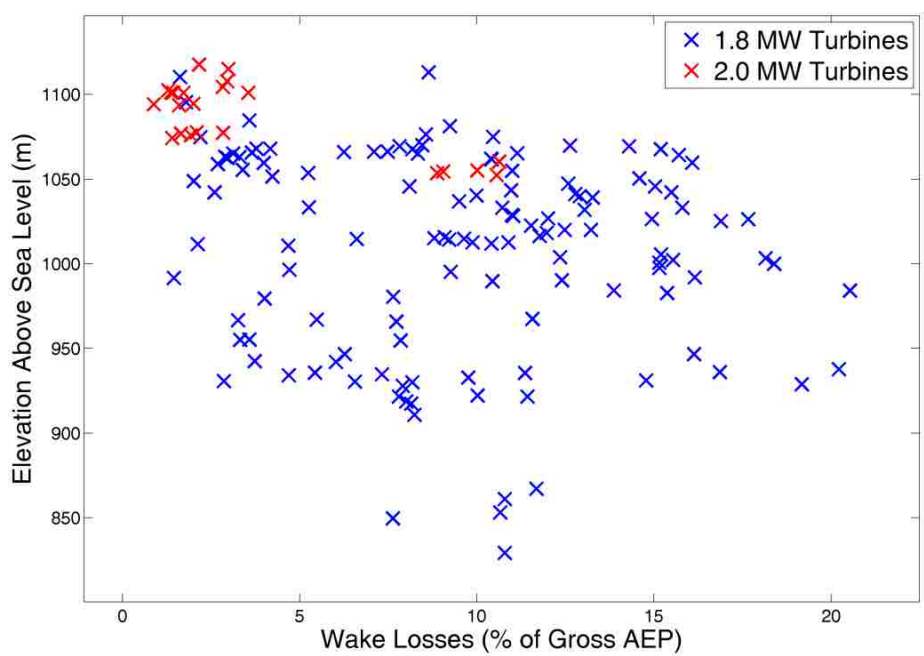


Figure 38 – Wake losses (% of gross AEP) with elevation above sea level (m). User correction for overestimations applied.

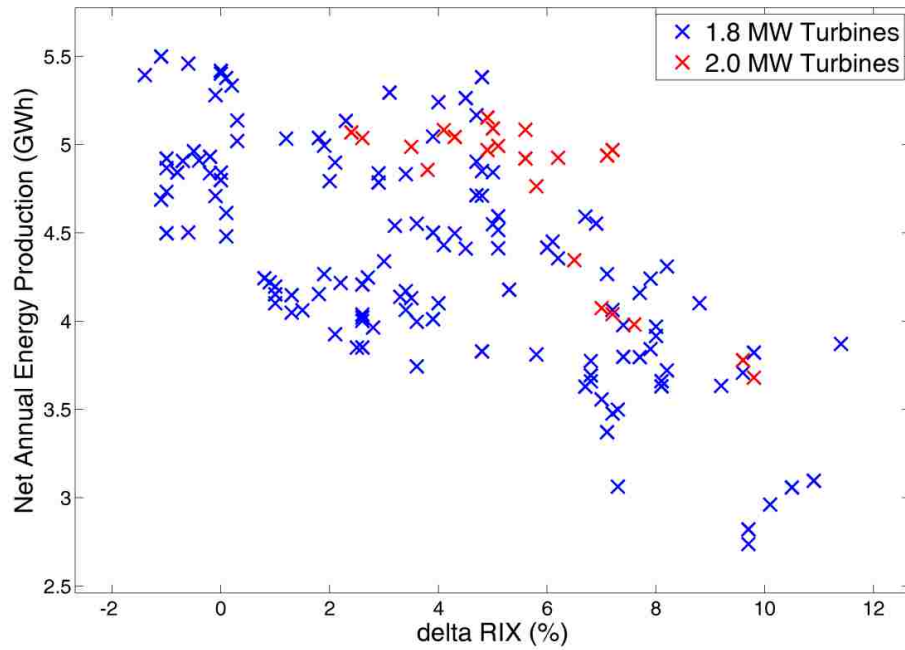


Figure 39 – Net AEP (GWh) with Δ RIX (%). User correction for overestimations applied.

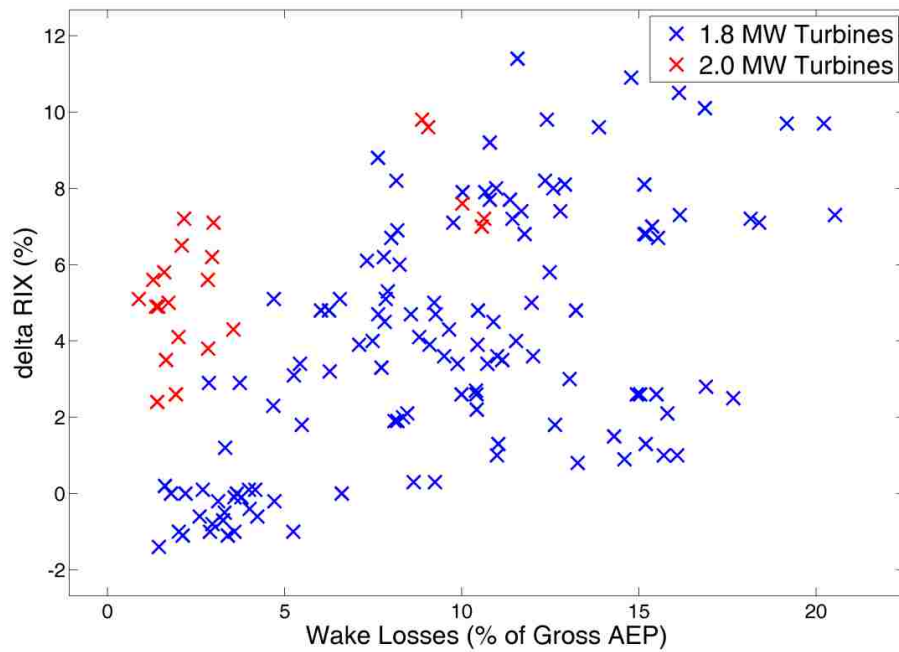


Figure 40 – Wake losses (% of gross AEP) with Δ RIX(%). User correction for overestimations applied.

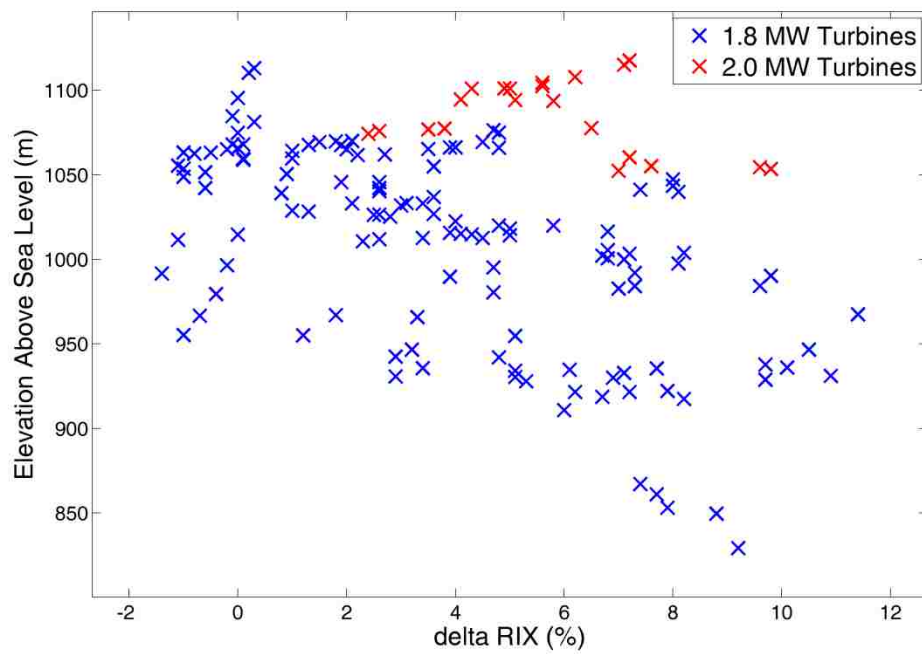


Figure 41 - Δ RIX(%) with elevation above sea level (m). User correction for overestimations applied.

Underestimation of Wind Speeds due to roughness of terrain

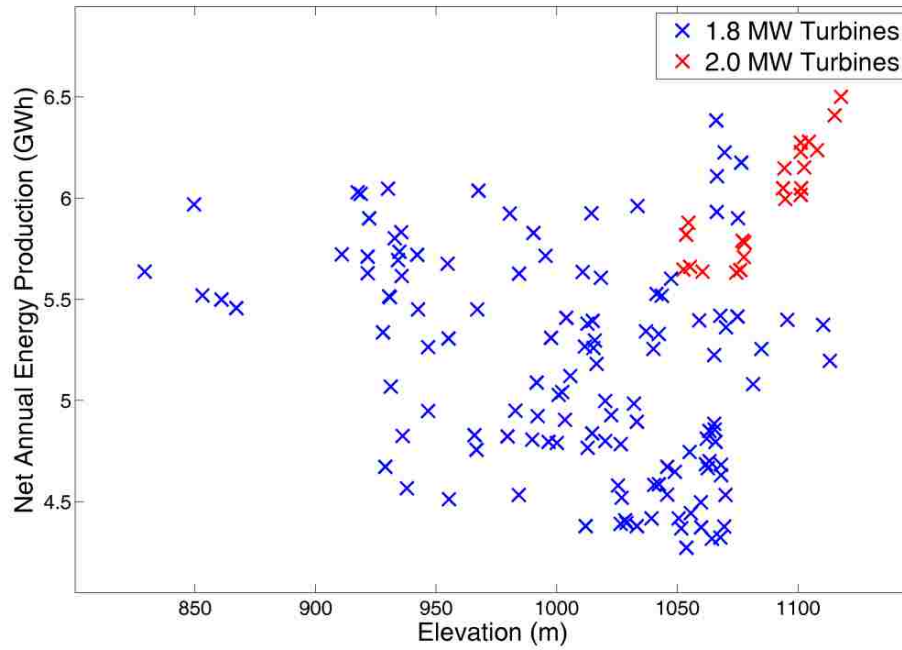


Figure 42 - Net AEP (GWh) with elevation above sea level (m). User correction for underestimations applied.

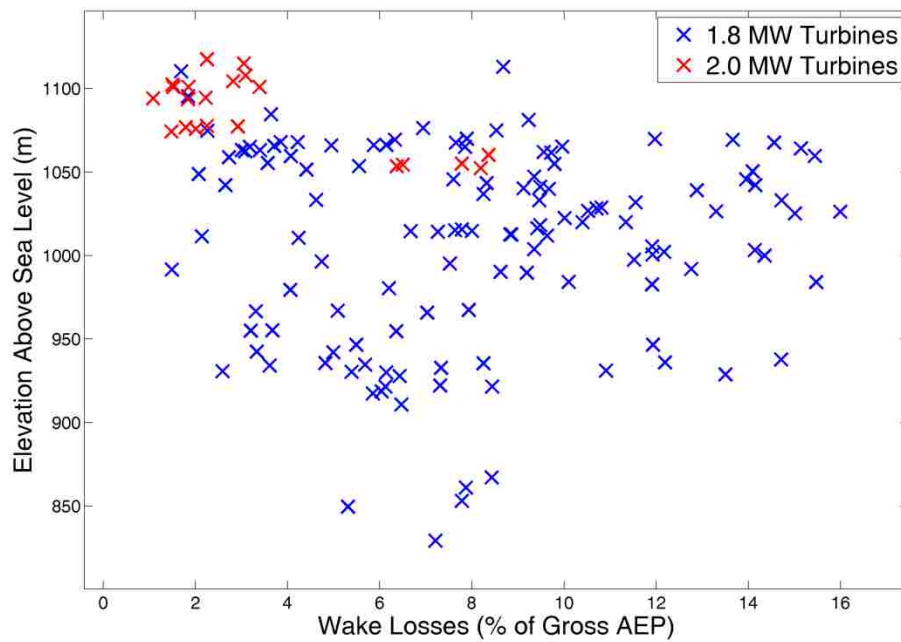


Figure 43 – Wake losses (% of gross AEP) with elevation above sea level (m). User correction for underestimations applied.

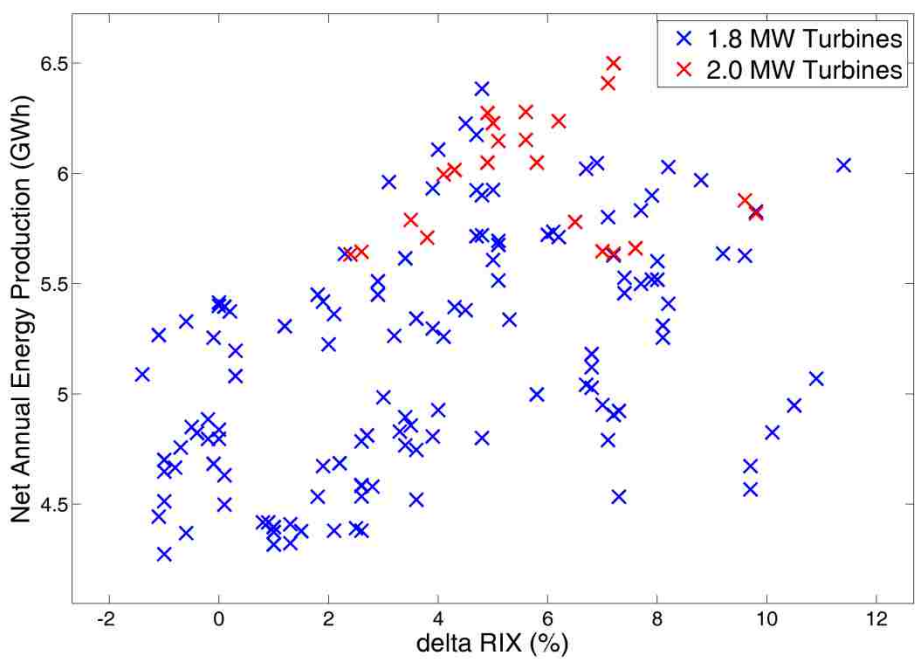


Figure 44 – Net AEP (GWh) with Δ RIX (%). User correction for underestimations applied.

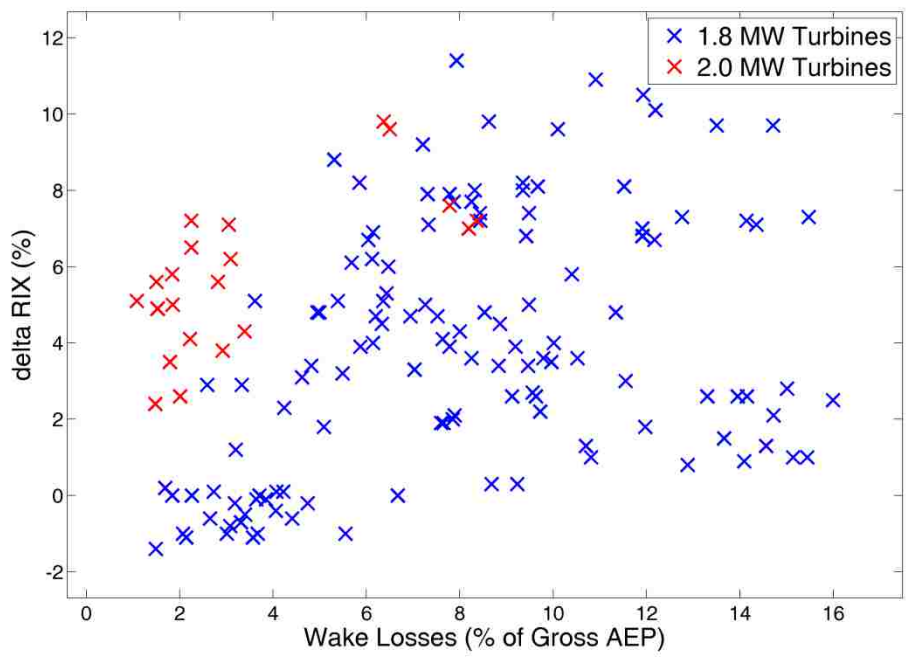


Figure 45 – Wake losses (% of gross AEP) with Δ RIX(%). User correction for underestimations applied.

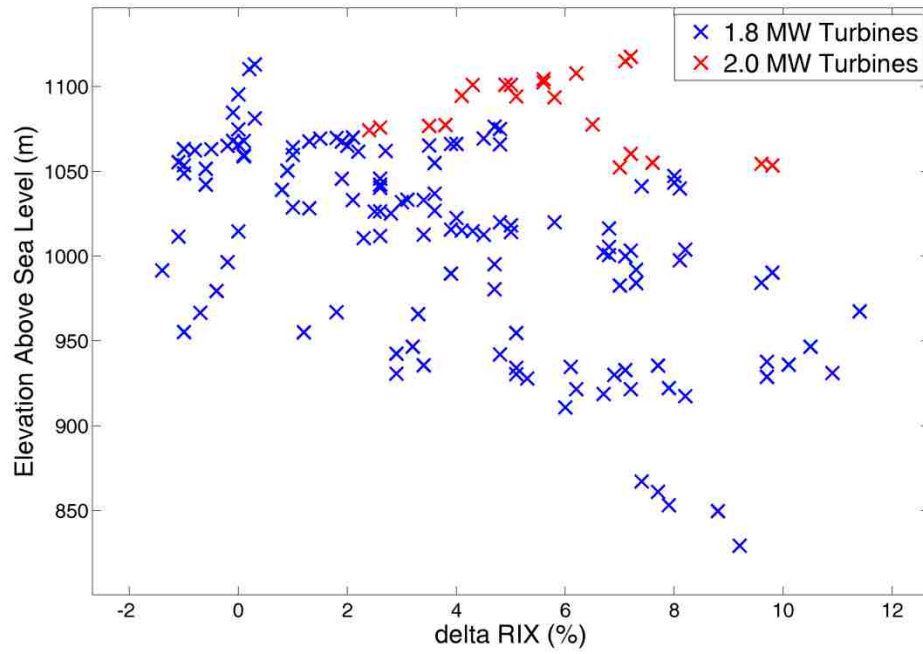


Figure 46 - Δ RIX(%) with elevation above sea level (m). User correction for underestimations applied.

Appendix B – Measured vs. Predicted Production

WAsP Predictions

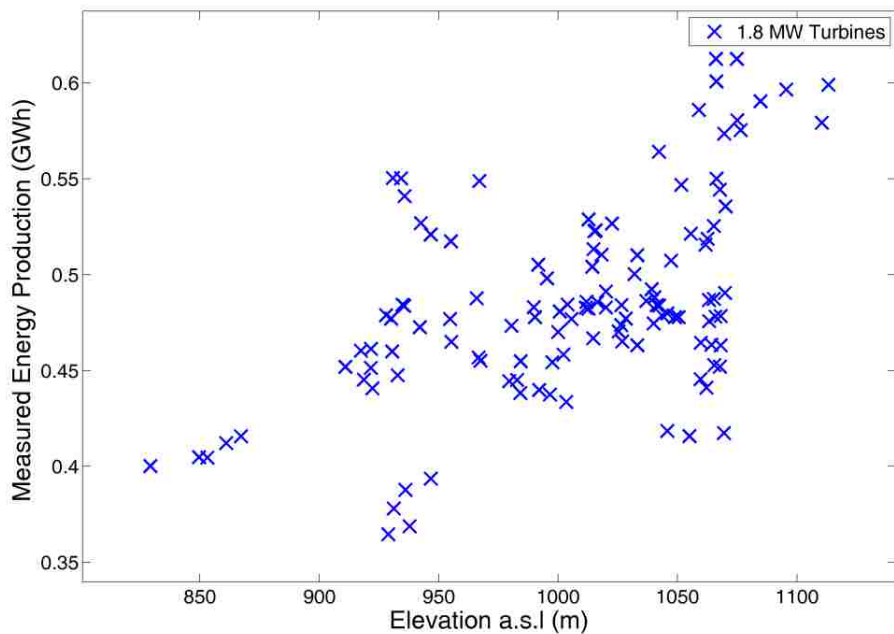


Figure 47 – Elevation above sea level (m) and Measured Production (GWh) for all 1.8 MW sites. No user corrections.

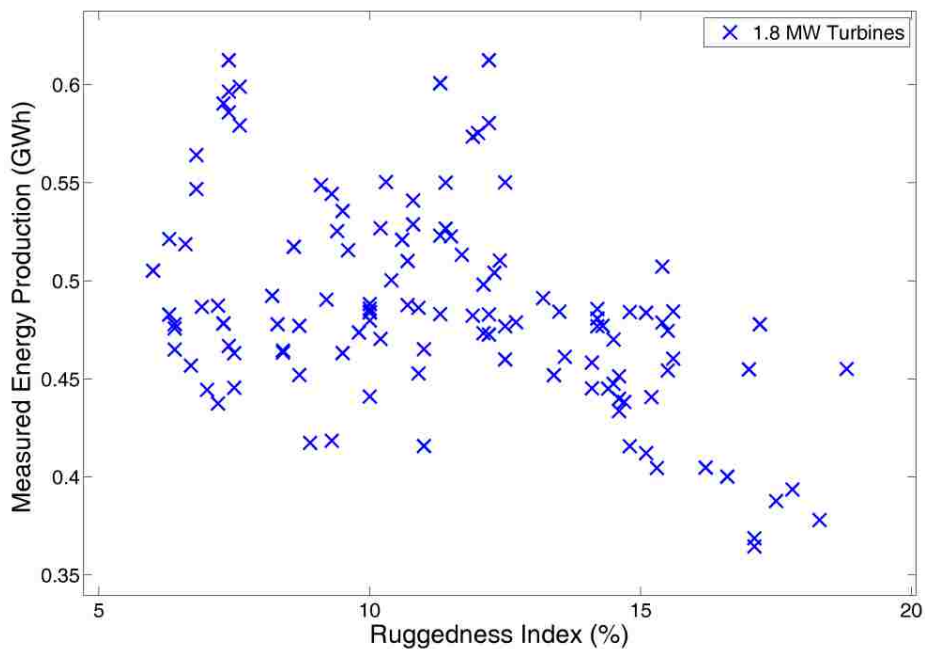


Figure 48 – Ruggedness Index (% of terrain exceeding critical slope) and Measured Production (GWh) for all 1.8 MW sites. No user corrections.

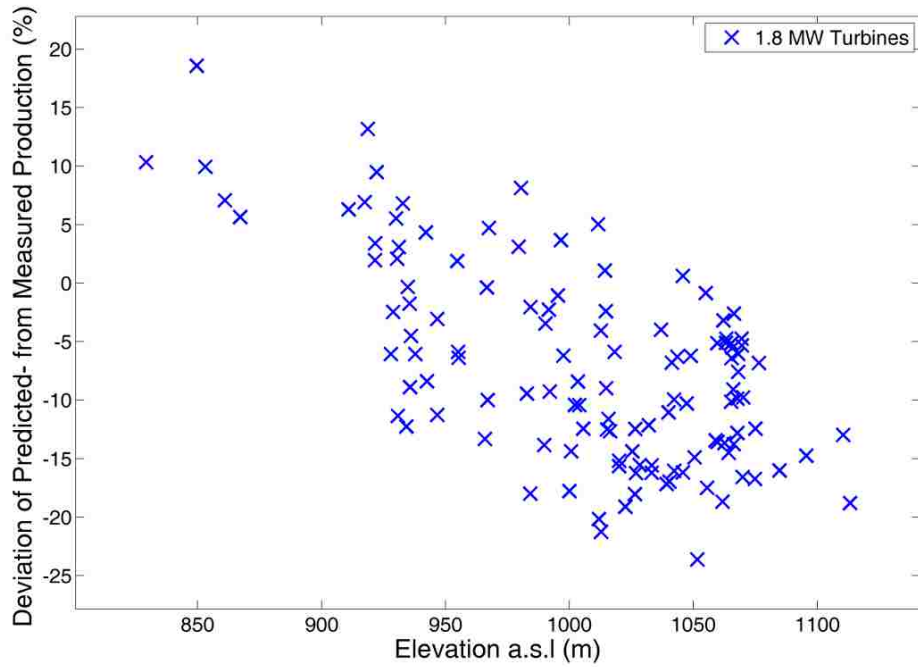


Figure 49 – Deviation of predicted from measured production (%) and elevation (m). No user corrections.

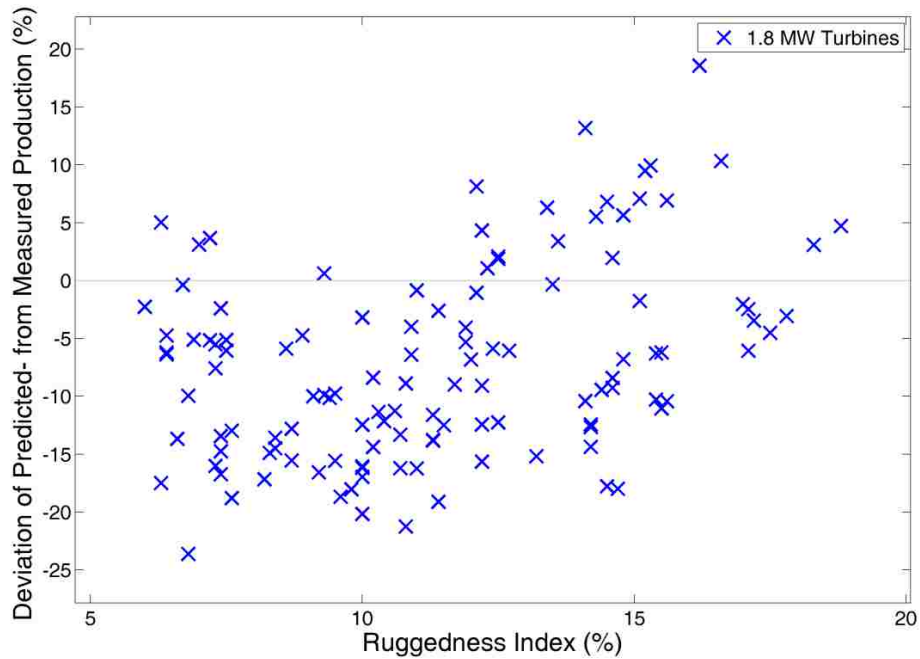


Figure 50 - Deviation of predicted from measured production (%) and Ruggedness Index (%).No user corrections.

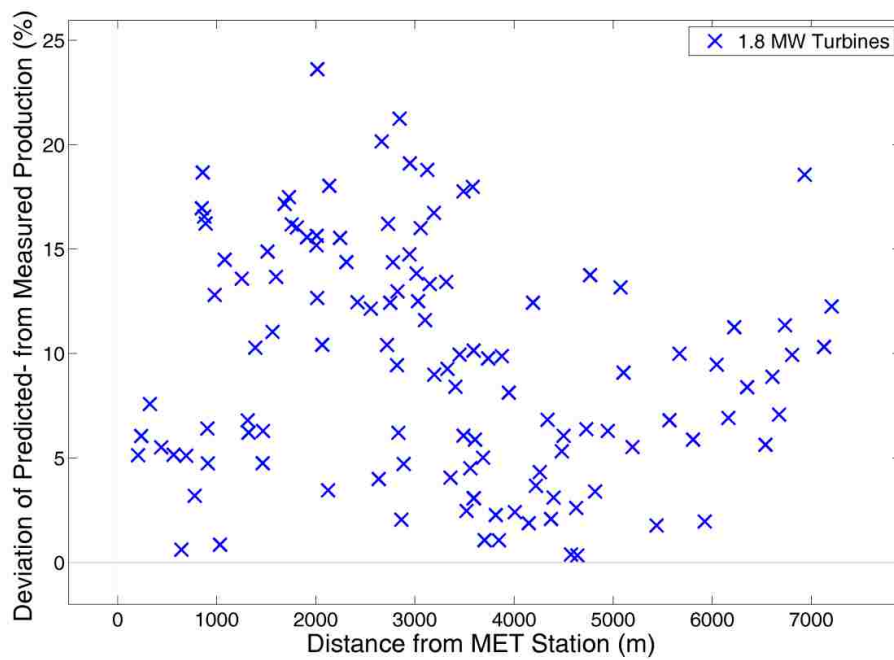


Figure 51 - Deviation of predicted from measured production (%) and Distance from MET station (%). No user corrections.

Overestimation of Wind Speeds due to roughness of terrain

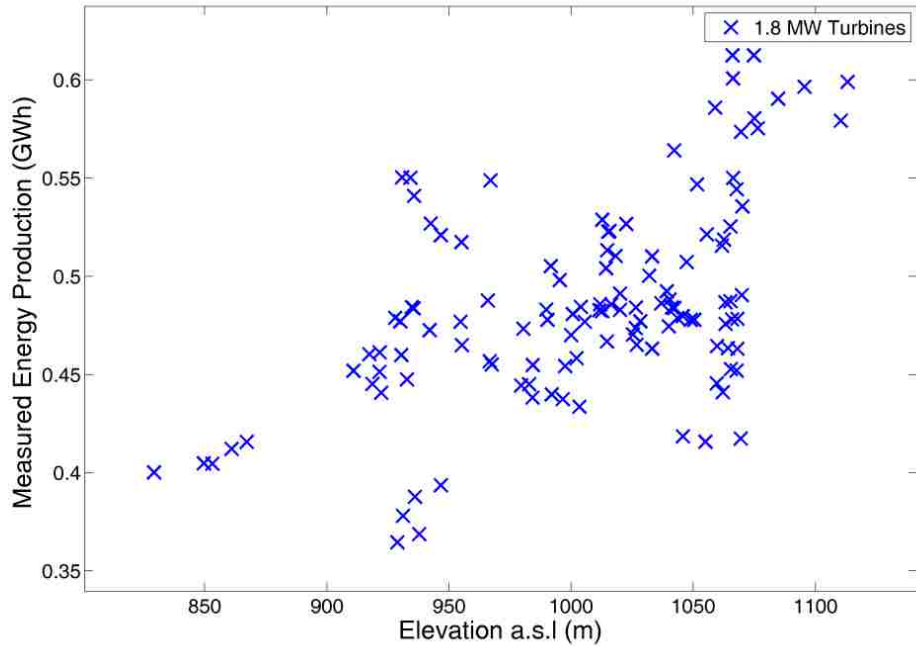


Figure 52 - Elevation above sea level (m) and Measured Production (GWh) for all 1.8 MW sites. User correction for overestimations applied.

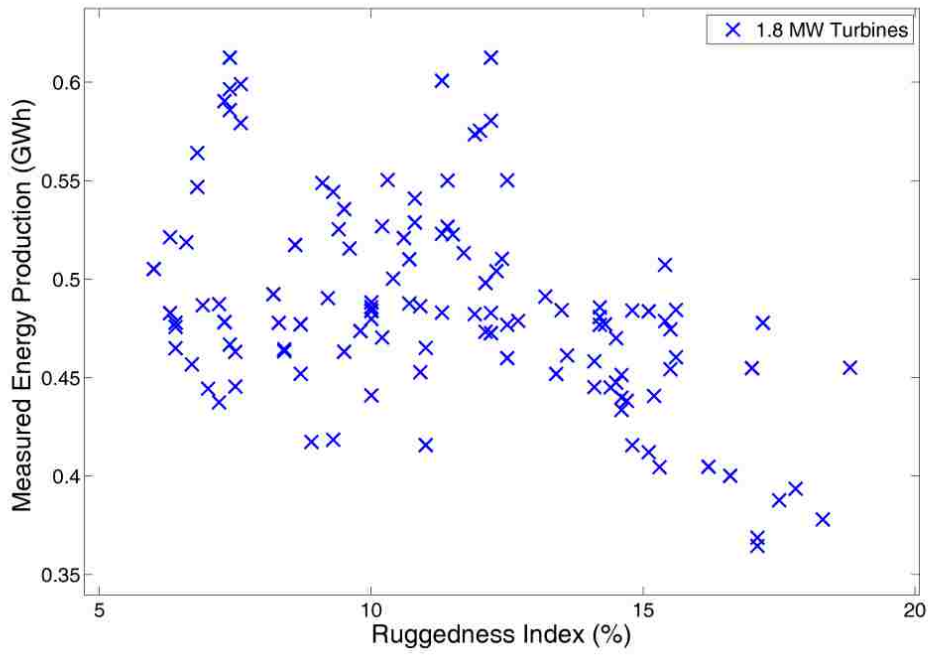


Figure 53 - Ruggedness Index (% of terrain exceeding critical slope) and Measured Production (GWh) for all 1.8 MW sites. User correction for overestimations applied.

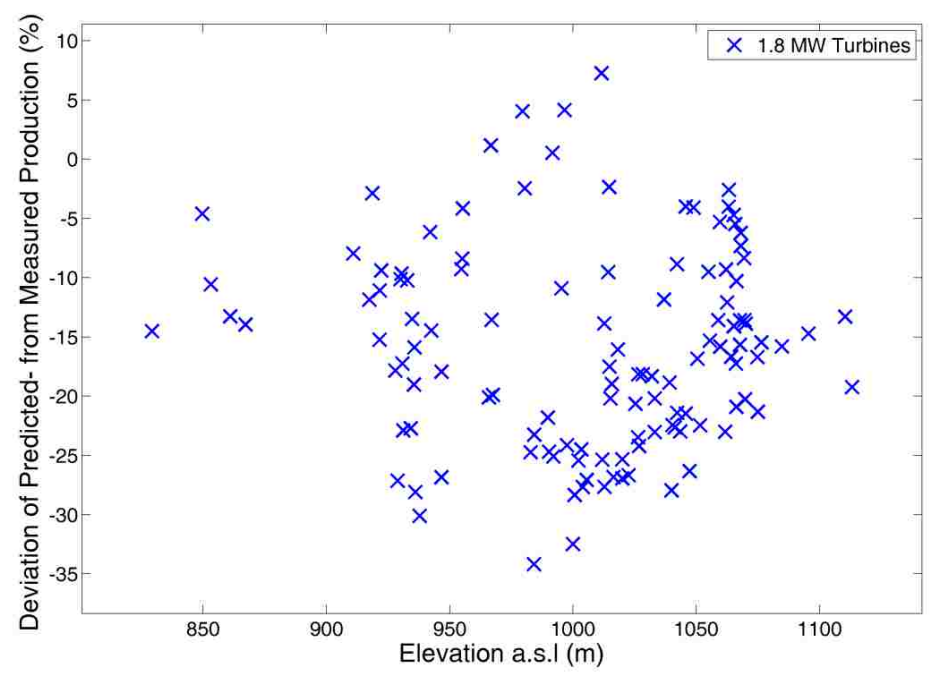


Figure 54 - Elevation above sea level (m) and Measured Production (GWh) for all 1.8 MW sites. User correction for overestimations applied.

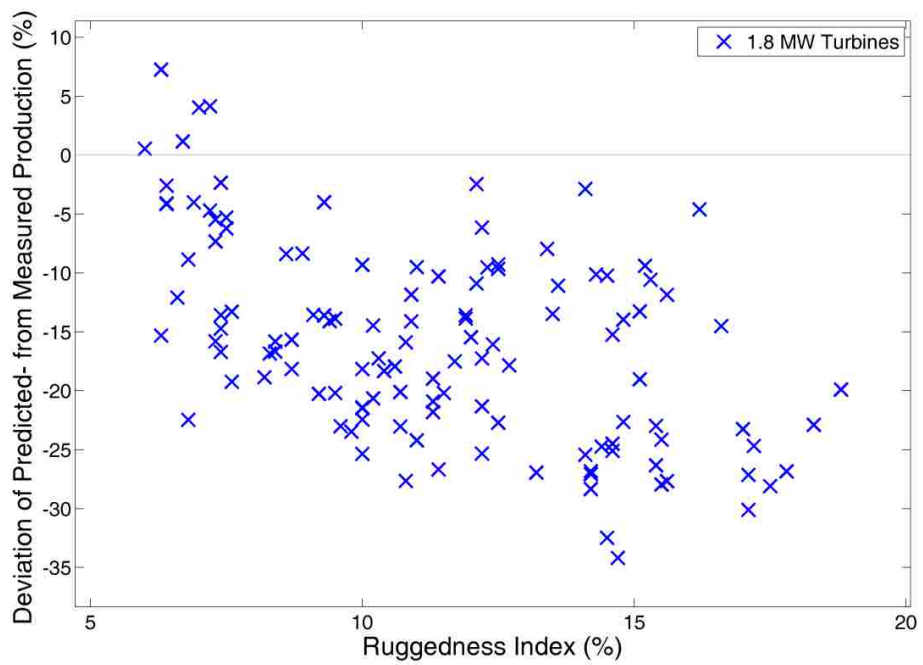


Figure 55 - Deviation of predicted from measured production (%) and Ruggedness Index (%). User correction for overestimations applied.

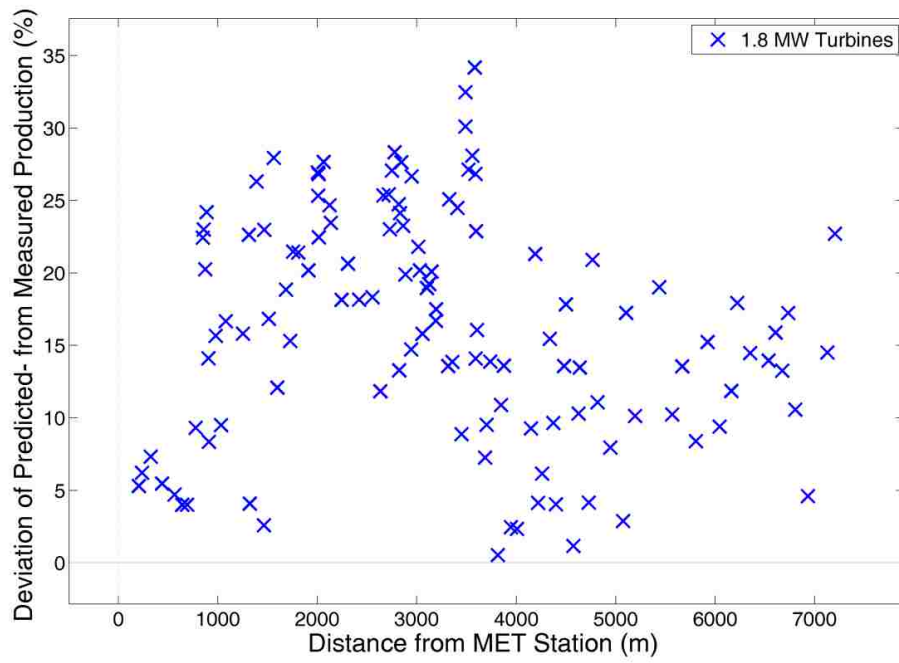


Figure 56 - Deviation of predicted from measured production (%) and Distance from MET station (%). User correction for overestimations applied.

Underestimation of Wind Speeds due to roughness of terrain

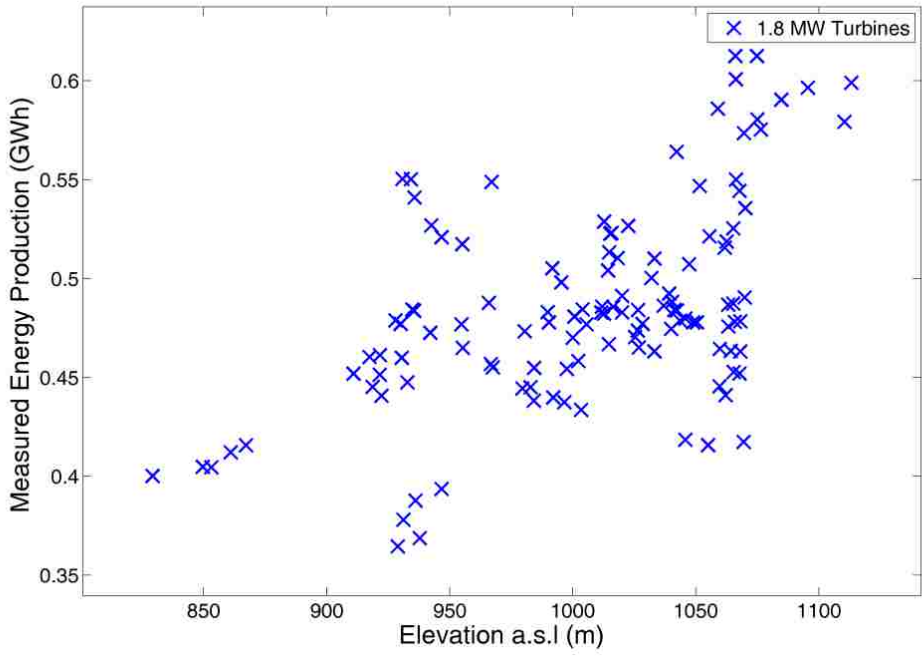


Figure 57 - Elevation above sea level (m) and Measured Production (GWh) for all 1.8 MW sites. User correction for underestimations applied.

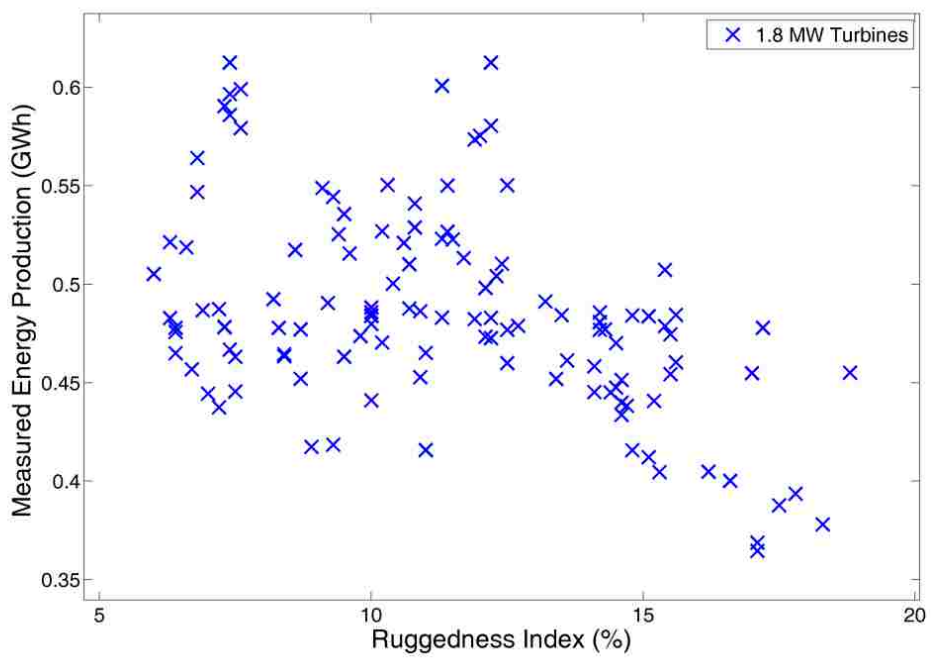


Figure 58 - Ruggedness Index (% of terrain exceeding critical slope) and Measured Production (GWh) for all 1.8 MW sites. User correction for underestimations applied.

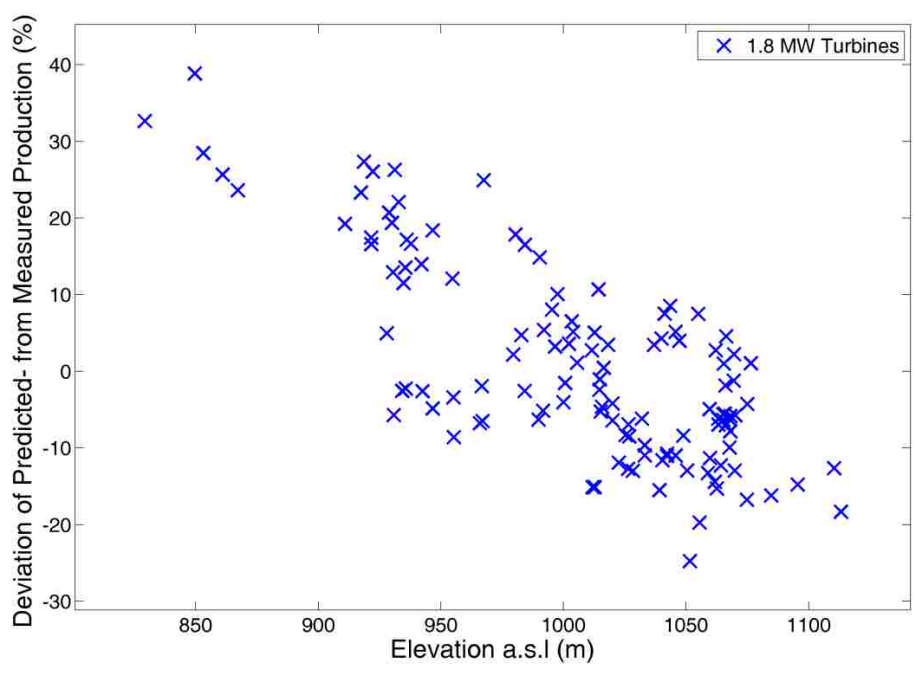


Figure 59 - Elevation above sea level (m) and Measured Production (GWh) for all 1.8 MW sites. User correction for underestimations applied.

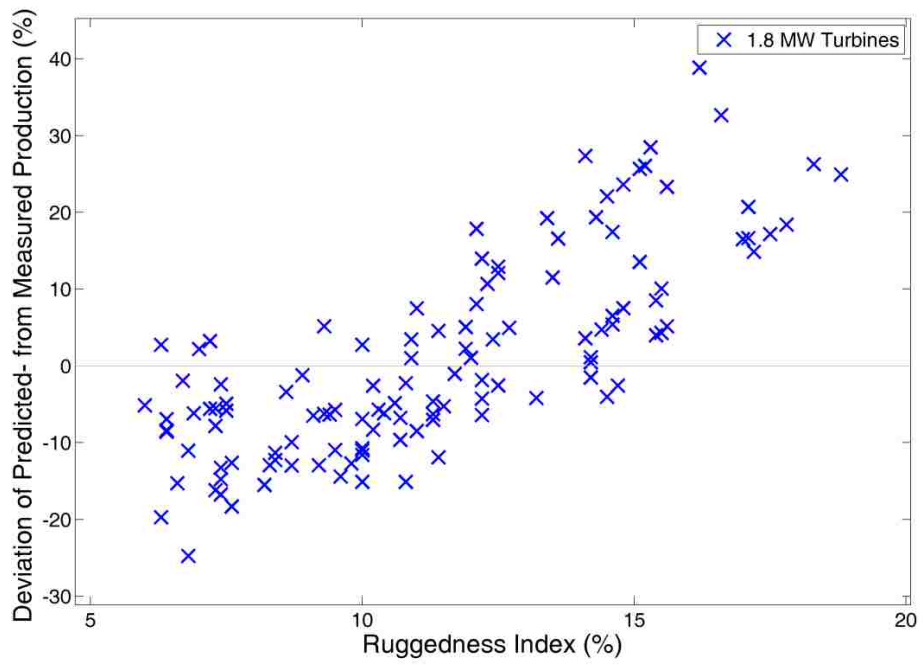


Figure 60 - Deviation of predicted from measured production (%) and Ruggedness Index (%). User correction for underestimations applied.

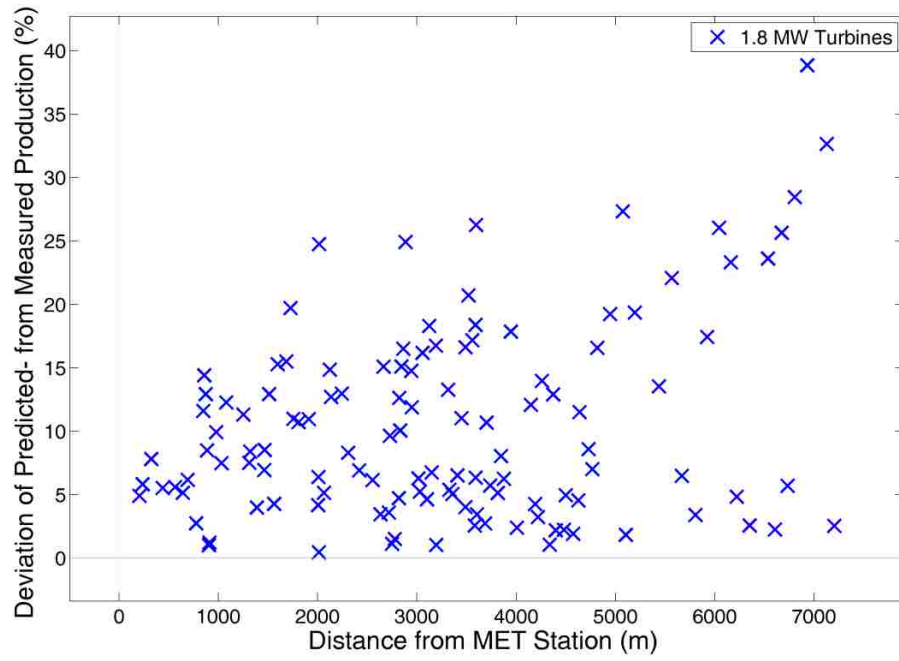


Figure 61 - Deviation of predicted from measured production (%) and Distance from MET station (%). User correction for underestimations applied.